



THE STUDY OF  $\alpha$  - PARTICLE INDUCED REACTIONS ON  
 $^{27}AL$  &  $^{197}AU$  NUCLIDES

By  
Ejigu Kebede

A THESIS SUBMITTED TO  
THE DEPARTMENT OF PHYSICS

PRESENTED IN PARTIAL FULFILLMENT OF THE REQUIREMENTS  
FOR THE DEGREE OF MASTER OF SCIENCE IN PHYSICS

ADDIS ABABA UNIVERSITY  
ADDIS ABABA, ETHIOPIA  
JUNE 2014

© Copyright by Ejigu Kebede,

ADDIS ABABA UNIVERSITY  
SCHOOL OF GRADUATE STUDIES

This is to certify that the thesis prepared by **Ejigu Kebede**, entitled “**THE STUDY OF  $\alpha$  - PARTICLE INDUCED REACTIONS ON  $^{27}Al$  &  $^{197}Au$  NUCLIDES**” and submitted in partial fulfillment of the requirements for the degree of **Master of Science in Physics** complies with the regulations of the University and meets the accepted standards with respect to originality.

Signed by the Examining Committee:

Examiner: Prof. P. Singh

Signature:\_\_\_\_\_Date:03 June 2014

Examiner: Dr. Tilahun Tesfaye

Signature:\_\_\_\_\_Date:03 June 2014

Advisor: Prof. A.K. Chaubey

Signature:\_\_\_\_\_Date:02 May 2014

ADDIS ABABA UNIVERSITY

Date: **June 2014**

Author: **Ejigu Kebede**

Title: **THE STUDY OF  $\alpha$  - PARTICLE INDUCED  
REACTIONS ON  $^{27}\text{Al}$  &  $^{197}\text{Au}$  NUCLIDES**

Department: **Physics**

Degree: **M.Sc.** Convocation: **June** Year: **2014**

Permission is herewith granted to Addis Ababa University to circulate and to have copied for non-commercial purposes, at its discretion, the above title upon the request of individuals or institutions.

---

Signature of Author

THE AUTHOR RESERVES OTHER PUBLICATION RIGHTS, AND NEITHER THE THESIS NOR EXTENSIVE EXTRACTS FROM IT MAY BE PRINTED OR OTHERWISE REPRODUCED WITHOUT THE AUTHOR'S WRITTEN PERMISSION.

THE AUTHOR ATTESTS THAT PERMISSION HAS BEEN OBTAINED FOR THE USE OF ANY COPYRIGHTED MATERIAL APPEARING IN THIS THESIS (OTHER THAN BRIEF EXCERPTS REQUIRING ONLY PROPER ACKNOWLEDGEMENT IN SCHOLARLY WRITING) AND THAT ALL SUCH USE IS CLEARLY ACKNOWLEDGED.

# Abstract

In this work  $\alpha$  particle induced reaction on Aluminium ( $^{27}\text{Al}$ ) and Gold ( $^{197}\text{Au}$ ) in different energy range have been studied. Excitation function for the reaction channels of the type  $^{27}_{13}\text{Al}(\alpha, n)^{30}_{15}\text{P}$ ,  $^{27}_{13}\text{Al}(\alpha, 2p)^{29}_{13}\text{Al}$ ,  $^{27}_{13}\text{Al}(\alpha, n+2p)^{28}_{13}\text{Al}$ ,  $^{27}_{13}\text{Al}(\alpha, \alpha + n)^{26}_{13}\text{Al}$ ;  $^{197}_{79}\text{Au}(\alpha, n)^{200}_{81}\text{Tl}$ ,  $^{197}_{79}\text{Au}(\alpha, 2p)^{199}_{79}\text{Au}$ ,  $^{197}_{79}\text{Au}(\alpha, n+2p)^{198}_{79}\text{Au}$  and  $^{197}_{79}\text{Au}(\alpha, \alpha + n)^{196}_{79}\text{Au}$  were studied and comparative analyses were made for analogous reaction channels of both the light  $^{27}\text{Al}$  and heavy  $^{197}\text{Au}$  target nuclei. The experimentally measured excitation functions obtained from EXFOR data source, IAEA, have been compared with the theoretical calculations with and without the inclusion of pre-equilibrium emission of particles, made by COMPLET code. Level density parameter is varied to get good agreement between the calculated and measured data with minimum effort on parameter fitting. In the study different reaction nature were observed between the heavy and light nuclides while being bombarded by the projectile of  $\alpha$  particle having the same energy range.

# Acknowledgement

Behind the screen of my successes there is one, the almighty God, who never let me alone in all my life journey. I thank him above all.

I would like to extend my deepest and sincere gratitude to my advisor Prof. A.K.Chaubey for his unreserved advise and support to realize this work. His values will not be ended by the accomplishment of my study but also will be continued to the rest of my life.

My strongest thank is intended to my family and my intimate friends.

# Contents

<b>Abstract</b>	<b>iv</b>
<b>Acknowledgement</b>	<b>v</b>
<b>1 Introduction</b>	<b>1</b>
<b>2 Theories of Nuclear Reaction</b>	<b>6</b>
2.1 Introduction . . . . .	6
2.1.1 Conservation laws . . . . .	7
2.1.2 Energetics of nuclear reactions . . . . .	8
2.1.3 Reaction cross sections ( $\sigma$ ) . . . . .	8
2.2 Reaction Mechanisms . . . . .	9
2.2.1 Direct Reaction Model . . . . .	11
2.2.2 Compound Nucleus Model . . . . .	13
2.2.3 The Optical Model . . . . .	15
2.2.4 Pre-equilibrium or pre-compound Model . . . . .	16
2.2.5 Other semi-classical models . . . . .	21
2.2.6 Interanuclear Cascade Model . . . . .	23
2.2.7 Heavy ion reactions . . . . .	23
<b>3 Computer Code COMPLET</b>	<b>25</b>
<b>4 Reaction Channels, Analysis and Discussion</b>	<b>31</b>
4.1 Reaction Channels . . . . .	31
4.1.1 Reaction Channels of $^{27}\text{Al}$ . . . . .	31
4.1.2 Reaction Channels of $^{197}\text{Au}$ . . . . .	33
4.2 Analysis and Discussion . . . . .	36
4.2.1 $^{27}_{13}\text{Al}(\alpha, n)^{30}_{15}\text{P}$ Reaction . . . . .	38
4.2.2 $^{197}_{79}\text{Au}(\alpha, n)^{200}_{81}\text{Tl}$ Reaction . . . . .	39
4.2.3 $^{27}_{13}\text{Al}(\alpha, n + 2p)^{28}_{13}\text{Al}$ Reaction . . . . .	41
4.2.4 $^{197}_{79}\text{Au}(\alpha, n + 2p)^{198}_{79}\text{Au}$ Reaction . . . . .	42
4.2.5 $^{27}_{13}\text{Al}(\alpha, 2p)^{29}_{13}\text{Al}$ Reaction . . . . .	43
4.2.6 $^{197}_{79}\text{Au}(\alpha, 2p)^{199}_{79}\text{Au}$ Reaction . . . . .	45
4.2.7 $^{27}_{13}\text{Al}(\alpha, \alpha + n)^{26}_{13}\text{Al}$ Reaction . . . . .	46
4.2.8 $^{197}_{79}\text{Au}(\alpha, \alpha + n)^{196}_{79}\text{Au}$ Reaction . . . . .	48

<b>5 Conclusion</b>	<b>50</b>
<b>References</b>	<b>52</b>

# Chapter 1

## Introduction

Nuclear data are quantitative results of scientific investigations of the nuclear properties of matter. They describe properties of atomic nuclei and the fundamental physical relationships governing their interactions, there by characterizing the physical processes underlying all nuclear technologies. This is why the measurement and calculations of the cross section of nuclear reactions as much accurate as possible and understanding of nuclear reaction mechanisms is an important issue.

The shape of the variation of reaction cross section with excitation energy (excitation function) reveals the reaction mechanisms. The process of production of new nuclei and elementary particles in collision of particles and nuclei is known as nuclear reaction. A general nuclear reaction can be expressed by:

$X + a \rightarrow Y + b + Q$ , where  $a$  is the bombarding particle (projectile), which strike a target  $X$  and produce the residual nucleus  $Y$  and outgoing particle  $b$ .  $Q$  is the energy released in the reaction; so that  $Q$  is positive for exoergic reactions and negative for endoergic reactions. A nuclear reaction is usually expressed in compact form as  $X(a, b)Y$ . Generally,  $a$  and  $b$  will be nucleons or light nuclei, but occasionally  $b$  will be a  $\gamma$  ray, in which case the reaction is called radiative capture.

We classify reactions in many ways. If the incident and outgoing particles are the same (and correspondingly  $X$  and  $Y$  are the same nucleus), it is a scattering process, elastic if  $Y$  and  $b$  are in their ground states and inelastic if  $Y$  or  $b$  is in an excited state (from which it will generally decay quickly by  $\gamma$  emission).[1,2] Meaning, if the internal states

of the two colliding systems do not change, we have elastic scattering and if one or both systems are excited in the exit channel, it is inelastic scattering.

In this thesis the alpha -particle is the projectile or the bombarding particle and Gold (Au) and Aluminum (Al) nuclei are the targets. The different reaction channels studied are:  ${}_{13}^{27}\text{Al}(\alpha, n){}_{15}^{30}\text{P}$ ,  ${}_{13}^{27}\text{Al}(\alpha, 2p){}_{13}^{29}\text{Al}$ ,  ${}_{13}^{27}\text{Al}(\alpha, n+2p){}_{13}^{28}\text{Al}$ ,  ${}_{13}^{27}\text{Al}(\alpha, \alpha + n){}_{13}^{26}\text{Al}$ ;  ${}_{79}^{197}\text{Au}(\alpha, n){}_{81}^{200}\text{Tl}$ ,  ${}_{79}^{197}\text{Au}(\alpha, 2p){}_{79}^{199}\text{Au}$ ,  ${}_{79}^{197}\text{Au}(\alpha, n+2p){}_{79}^{198}\text{Au}$  and  ${}_{79}^{197}\text{Au}(\alpha, \alpha + n){}_{79}^{196}\text{Au}$ .

The objective of this thesis is to investigate the mechanisms of alpha-particle induced reaction on Gold (Au), heavy nuclide, and Aluminum (Al), light nuclide, with various projectile energies which is analysed with the help of computer code COMPLET. The reaction cross section for each channel mentioned above was analysed. The comparative analyses of the cross sections among the two target nuclides were conducted. The different channels are the results of the projectile energies.

For many years it was assumed that all types of nuclear reactions takes place in two stages, a direct stage that occurs in the time it takes a projectile to cross the target nucleus which is about  $10^{-22}$ s and a compound nucleus stage when emission takes place from equilibrated nucleus. The direct reaction which includes the stripping and pick-up reactions are characterized by certain angular distributions of the scattered or the outgoing particles. Those particles can be understood by regarding the reactions as having involved only the interaction between the incident particle and the outer nucleons of the target nucleus. The second stage of nuclear reaction (compound nucleus) is historically proposed by Niles Bohr. The initiation to develop the compound nucleus theory is the problem for resonance peak of nuclear reactions. According to this theory the sharp peak of the reaction cross section is due to the existence of the quasi-stable nuclear state for particular value of resonance energy.

Another evidence for the compound nucleus theory is the heavy ion induced reaction. Heavy ion induced reactions with projectile energy closed to coulomb barrier are dominated by compound nucleus and direct reactions. As the projectile energy is increased compound nucleus formation is hindered and incomplete fusion starts competing with the complete fusion. More extensive measurements show that some cross sections cannot be explained using the direct and compound reactions models. This shows that particles are emitted after the direct stage but prior to the establishment of statistical equilibrium, which is the compound nucleus stage. This new stage is given a name pre-equilibrium reaction stages. To explain this theory different pre-equilibrium nuclear reaction models have been developed. The first model developed by J.J Griffn was the exciton model. The model was further modified and developed by M.Blanand et al. In the pre-equilibrium theories of nuclear reaction it is assumed that interaction is due to successive nucleon-nucleon interaction in a series of stages. Each interaction produces a particle-hole (p - h) pair and the particle-hole pair is called an exciton. Certain nuclear reactions can be explained using a quantum mechanical approach provided that the projectile is not a complex particle like heavy ion. The alpha-particle-induced reaction is a semi classical treatment. That is the angular distributions are treated quantum mechanically and the forward motion classically.

The second chapter of this thesis covers discussions on the theories of nuclear reaction mechanisms and reaction models in general. Nuclear model codes are helpful in the validation of existing data; they can also generate an evaluation that is entirely complete in its description of reaction channels, incident and outgoing particle energies and angles. The adjustable parameters of the nuclear model code should be fitted to reproduce the experimental data in the process of evaluation. The most important parameters are: optical model parameters, level density parameters, gamma ray transmission coefficients, equilibrated emissions, direct interactions, pre-equilibrium reactions and multiple emissions of particles. Hence in chapter three of the thesis the computer code COMPLET is discussed.

COMPLET computer code is among the many computer codes available to compute the pre-equilibrium and equilibrium excitation functions. Analysis of reaction cross sections as a function of energy (excitation function) for the alpha-particle-induced reaction on Aluminum and Gold nuclei at different channels of different projectile energies were analyzed with the calculations obtained using this computer code. The theoretical results were compared with the experimental data obtained from EXFOR data source, IAEA. These are plotted together for comparison. Parallel analysis was done for both the light nucleus  $^{27}\text{Al}$  and heavy nucleus  $^{197}\text{Au}$  and the result was compared and commented accordingly.

The EXFOR database is a large collection of experimental nuclear reaction data for incident neutrons, charged particles and photons. The EXchange FORmat was designed to be very flexible in order to be able to store the data as published. However, this flexibility is a drawback for systematic comparison of EXFOR data with evaluated data or nuclear reaction code results. At present, EXFOR is by far the most important and complete experimental nuclear reaction database with more than 130,000 data sets from about 19,000 experiments performed since 1935.[3] The database mainly contains numerical data and experimental/bibliographic information on low to medium energy experiments (up to 1 GeV) for incident neutron, charged particle, heavy ions and photon-induced reactions on a wide range of isotopes, natural elements, and compounds.[4]

In chapter four the reaction channels on which the thesis work relied is being analysed and discussed. The last chapter of this thesis is the conclusion and summary part where the main results are discussed and a brief summary is given.

**Gold** is a chemical element with the symbol Au and atomic number 79. It is a dense, soft, malleable, and ductile metal with an attractive, bright yellow color and luster that is maintained without tarnishing in air or water. Chemically, gold is a transition metal and a group 11 element. It is one of the least reactive chemical elements, solid under standard conditions. The metal therefore occurs often in free elemental (native) form, as nuggets

or grains in rocks, in veins and in alluvial deposits. Less commonly, it occurs in minerals as gold compounds, such as with tellurium as calaverite, sylvanite and krennerite. Gold has only one stable isotope,  $^{197}\text{Au}$ , which is also its only naturally occurring isotope. Thirty-six radioisotopes have been synthesized ranging in atomic mass from 169 to 205. The most stable of these is  $^{195}\text{Au}$  with a half-life of 186.1 days. The least stable is  $^{171}\text{Au}$ , which decays by proton emission with a half-life of  $30\mu\text{s}$ . Most of gold's radioisotopes with atomic masses below 197 decay by some combination of proton emission,  $\alpha$  decay, and  $\beta^+$  decay. The exceptions are  $^{195}\text{Au}$ , which decays by electron capture, and  $^{196}\text{Au}$ , which decays most often by electron capture (93%) with a minor  $\beta^-$  decay path (7%). All of gold's radioisotopes with atomic masses above 197 decay by  $\beta^-$  decay. At least 32 nuclear isomers have also been characterized, ranging in atomic mass from 170 to 200. Within that range, only  $^{178}\text{Au}$ ,  $^{180}\text{Au}$ ,  $^{181}\text{Au}$ ,  $^{182}\text{Au}$ , and  $^{188}\text{Au}$  do not have isomers. Gold's most stable isomer is  $^{198m_2}\text{Au}$  with a half-life of 2.27 days. Gold's least stable isomer is  $^{177m_2}\text{Au}$  with a half-life of only 7ns.  $^{184m_1}\text{Au}$  has three decay paths:  $\beta^+$  decay, isomeric transition, and  $\alpha$  decay. No other isomer or isotope of gold has three decay paths.[5]

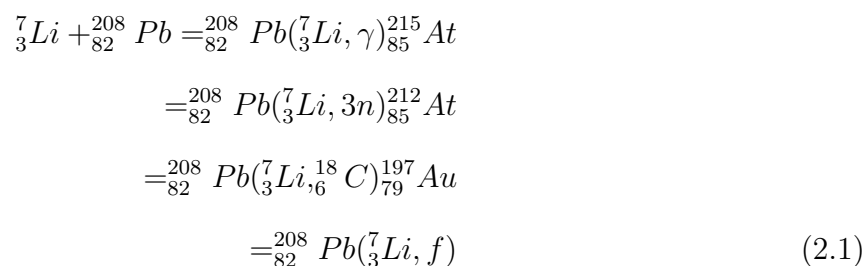
**Aluminum** has many known isotopes, whose mass numbers range from 21 to 42; however, only  $^{27}\text{Al}$  (stable isotope) and  $^{26}\text{Al}$  (radioactive isotope,  $t_{1/2} = 7.2 \times 10^5 \text{yrs}$ ) occur naturally.  $^{27}\text{Al}$  has a natural abundance above 99.9%.  $^{26}\text{Al}$  is produced from argon in the atmosphere by spallation caused by cosmic-ray protons. Aluminum isotopes have found practical application in dating marine sediments, manganese nodules, glacial ice, quartz in rock exposures, and meteorites.[6] Aluminum has a wide range of uses in industrial, domestic consumer, and medical products. Its nuclear data, in particular, are necessary for design of an accelerator-based facility to produce radioisotopes, including analyses of system performance, induced radiation doses, and material activation, as well as heating, damage, and shielding requirements.[7]

# Chapter 2

## Theories of Nuclear Reaction

### 2.1 Introduction

A nuclear reaction occurs when a projectile strikes a target nucleus [8]. A nuclear reaction can be defined as a collision between two nuclei that produces a change in the nuclear composition and/or the energy state of the interacting species. A reaction involves a projectile, a nucleus that is produced in a particle accelerator or nuclear reactor. The projectile is incident upon a target nucleus, which is usually fixed ( $v = 0$ ), but in some accelerators colliding beams are possible, thereby increasing the center-of-mass energy of the collision. The products of a reaction may include any possible nuclei that are permitted by the conservation laws (mass-energy, baryons, charge, parity etc.). By accelerating the projectile, kinetic energy can be converted to mass in order to overcome negative Q-values. The notation for nuclear reactions is: *Target(projectile, lightproducts)heavyproduct(s)*. As example, consider the following reaction and several possible products:



where f indicates fission

### 2.1.1 Conservation laws

In analysing nuclear reactions several conservation laws will be applied. Some of these include:

i. **Conservation of total energy and linear momentum:** - which can be used to relate the unknown but perhaps measurable energies of the products to the known and controllable energy of the projectile. We can thus use the measured energy of ejectile to deduce the excitation energy of states of the product or the mass difference between the target and the product.

ii. **Conservation of proton and neutron number (conservation of charge and mass number):**- is a result of the low energy of the process, in which no meson formation or quark rearrangement take place. At higher energies we still conserve total nucleon number, but at low energy we conserve separately proton number and neutron number.

iii. **Conservation of parity:**- also applies the net parity before the reaction must equal the net parity after the reaction. If we know the orbital angular momentum of the outgoing particle, we can use the  $(-1)^l$  rule and the other known parities in the reaction to deduce unknown parities of excited states.

iv. **Conservation of spin:**- spin or "Angular momentum" is a quantity which measures how quickly an object is rotating or revolving about a fixed line called an axis. It enables us to relate the spin alignments of the reacting particles and the orbital angular momentum carried by the outgoing particle, which can be deduced by measuring its angular distribution. Classically, it is given by the product  $mrv$  of the mass of the object, its distance from the axis, and its velocity perpendicular to the line between it and the axis. The conservation of angular momentum is related to the fact that the laws of physics don't depend on the orientation of particular coordinate system.

### 2.1.2 Energetics of nuclear reactions

Conservation of total relativistic energy in our basic reaction gives

$$m_x c^2 + T_x + m_a c^2 + T_a = m_y c^2 + T_y + m_b c^2 + T_b \quad (2.2)$$

Where the T's are kinetic energies (for which we can use the non-relativistic approximation  $\frac{1}{2}mv^2$  at low energy) and the m's are rest masses. We define the reaction Q value, in analogy with radioactive decay Q values, as the initial mass energy minus the final mass energy:

$$\begin{aligned} Q &= (m_{initial} - m_{final})c^2 \\ &= (m_x + m_a - m_y - m_b)c^2 \end{aligned} \quad (2.3)$$

which is the same as the excess kinetic energy of the final products:

$$\begin{aligned} Q &= T_{final} - T_{initial} \\ &= T_y + T_b - T_x - T_a \end{aligned} \quad (2.4)$$

The Q value may be positive, negative, or zero. If  $Q > 0$  ( $m_{initial} > m_{final}$  or  $T_{final} > T_{initial}$ ) the reaction is said to be exoergic or exothermic: in this case nuclear mass or binding energy is released as kinetic energy of the final products, When  $Q < 0$  ( $m_{initial} < m_{final}$  or  $T_{final} < T_{initial}$ ) the reaction is endoergic or endothermic, and initial kinetic energy is converted into nuclear mass or binding energy. The changes in mass and energy must of course be related by the familiar expression from special relativity.  $\Delta E = \Delta mc^2$  any change in the kinetic energy of the system of reacting particles must be balanced by an equal change in its rest energy.[2]

### 2.1.3 Reaction cross sections ( $\sigma$ )

Nuclear reaction cross section is the measurement of probability of the reaction. This is defined in terms of number of events produced (number of particles emitted after reaction) for specific number of incident particle or it can also defined interms of number of nuclei transformed per specific number of incident particles. The Nuclear reaction cross section

is the effective area of the nuclei shown to the incident beam or it is the effective area of the nuclei as seen by the incident beam. Or roughly speaking, [2] the cross section is a measure of the relative probability for the reaction to occur. This is represented by:

$$\sigma = \frac{\text{Number of particular types of events per unit time per nuclei}}{\text{Number of incident particles per unit time per unit area}} \quad (2.5)$$

The geometric cross-section that a nucleus presents to a beam of particles is  $\pi r^2$ . If we use  $6 \times 10^{-15}m$  as an average value for the nuclear radius, the value of  $\pi r^2$  becomes  $3.14(6 \times 10^{-15})^2 \approx 10^{-28}m^2$ . This geometric cross-section of nuclei is reflected in the unit of reaction probability which is the barn, where  $1b = 10^{-28}m^2$ . The cross section is directly related to the difference between the final and initial nuclear states and does not involve the states of all the other nucleons.[9] The study of the cross sections of the nuclear reaction is important for two reasons:[10]

- i. For empirical knowledge for various applied purposes, e.g. in fission or fusion studies required for designing reactors or for various fission devices.
- ii. For understanding the reaction mechanism.

## 2.2 Reaction Mechanisms

Nuclear reactions, like chemical reactions, can occur via different reaction mechanisms.

There are various reaction mechanism models. Some of these are:

- i. Direct reaction model
- ii. Compound nucleus model
- iii. Optical model
- iv. Pre-equilibrium or pre-compound model
- v. Other semi-classical models
- vi. Interanuclear Cascade Model
- vii. Heavy ion reactions

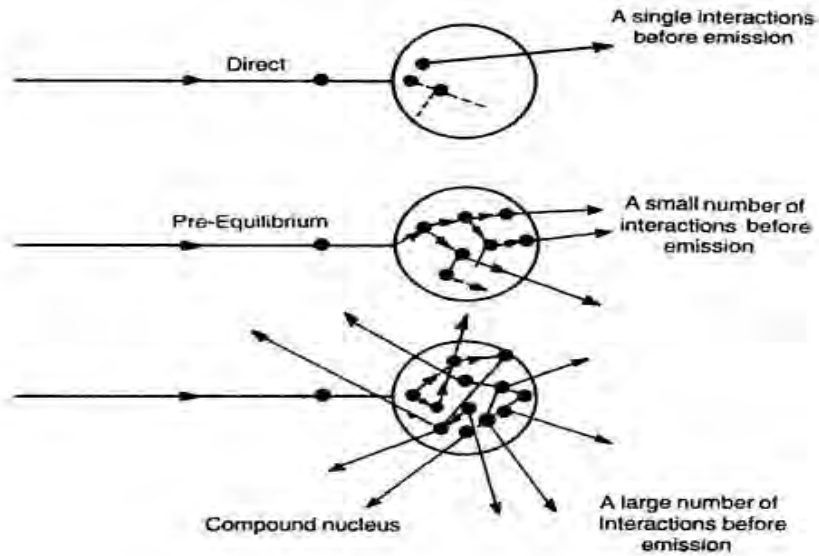


Fig.2.1 The three modes of reaction mechanism.

Weisskopf has presented a simple conceptual model (fig. 2.2) for illustrating the relationships between the various nuclear reaction mechanisms.

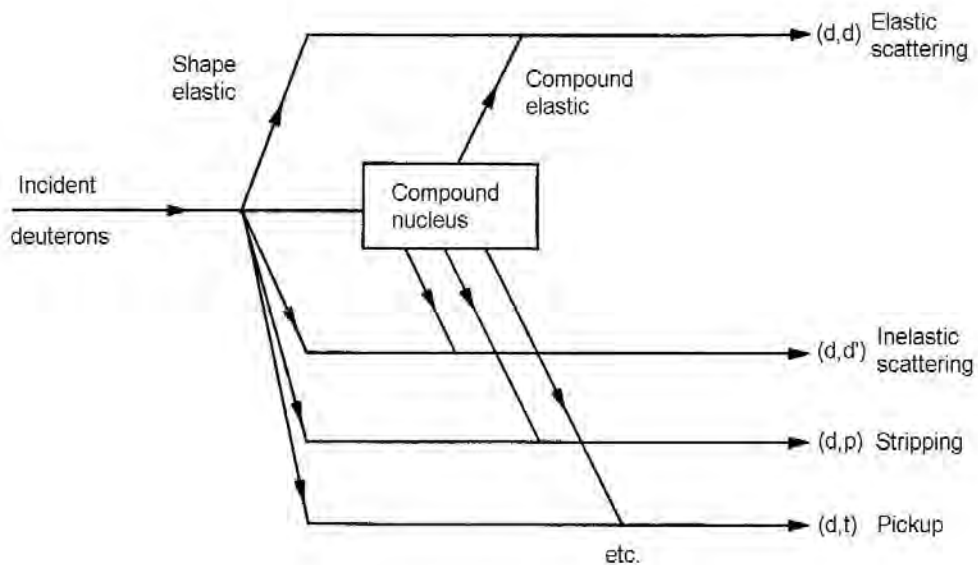


Fig. 2.2 Schematic illustration showing two types of reactions, direct and compound nucleus (modified from Hodgson 1971). Reactions can proceed directly, via compound nucleus, or both.

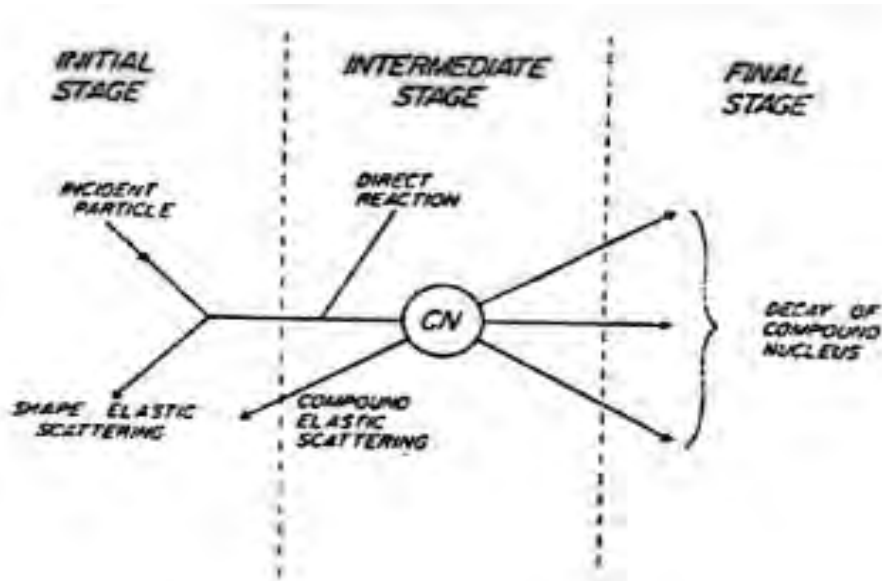


Fig.2.3 A conceptual view of the stages of nuclear reaction.[11]

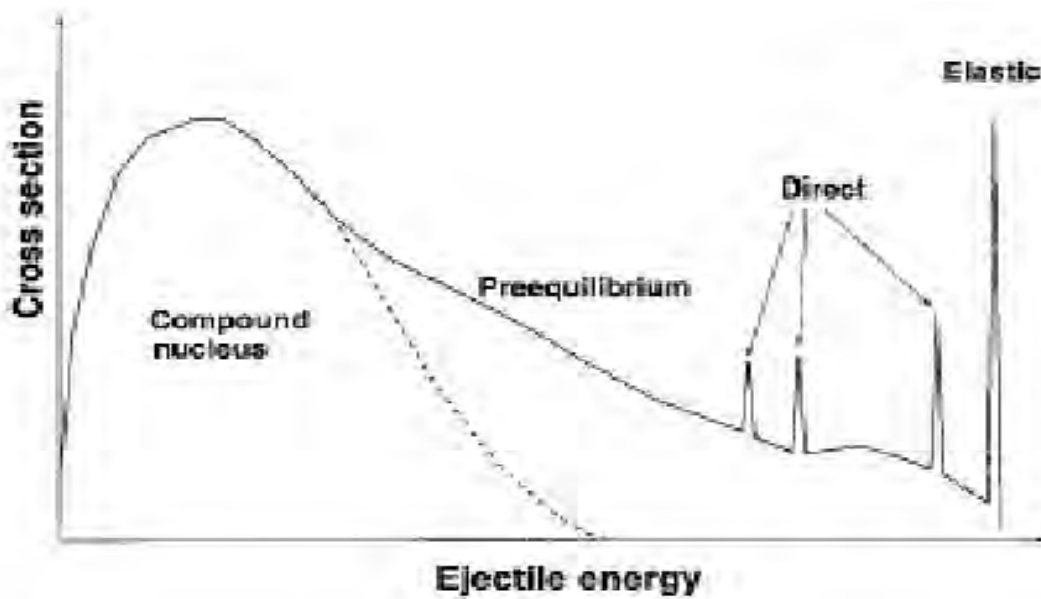


Fig.2.4 Neutron emission spectrum showing contributions of different reaction mechanisms in a nuclear reaction.

### 2.2.1 Direct Reaction Model

If the nuclear reactions proceed directly from the entrance channel to the exit channel without the formation of an intermediate state, they are said to be direct reactions. The indications of the direct reaction mechanism are: (i) the forward peaking in the angular

distributions of the outgoing particles and (ii) the short lifetimes of the composite system.[10] The direct reactions take place in the time the projectile takes to traverse the target nucleus (typically around  $10^{-22}s$ ). In these processes the projectile may interact with a nucleon, a group of nucleons or the whole nucleus and emission takes place immediately. The simplest direct reaction is elastic scattering, which leaves the target nucleus in its ground state.[8] They occur as a result of the interaction of the projectile with a specific degree of freedom, either of a single nucleon or a collective coordinate, causing that single degree of freedom to change. The projectile there upon escapes without further change to itself or the target.

In direct reactions (of which transfer reactions are an important subgroup), only very few nucleons take part in the reaction, with the remaining nucleons of the target serving as passive spectators. Such reactions might insert or remove a single nucleon from a shell-model state and might therefore serve as ways to explore the shell structure of nuclei.[2] The elastic cross-section depends on whether or not the scattering is due to long-range Coulomb interactions or to short-range strong interactions. The differential cross-section between two isolated charged particles diverges at small angles like  $\frac{d\sigma}{d\Omega} \propto \theta^{-4}$ . The total elastic cross-section is therefore infinite. For practical purposes, this divergence is eliminated because the Coulomb potential is screened at large distances by oppositely charged particles in the target.[12]

In non-elastic reactions, the states of the residual nuclei which are excited have a simple structural relationship with the ground state of the target nucleus. Inelastic scattering predominantly excites collective states, one nucleon transfer reactions excite single-particle states, and multinucleon transfer excites cluster states.[8] Inelastic reactions with no Coulomb barrier have cross-section dependences at low energy that depend on whether the reaction is exothermic or endothermic. Exothermic reactions generally have cross-section proportional to the inverse of the relative velocity,  $\sigma \propto \frac{1}{v}$ .[12]

## 2.2.2 Compound Nucleus Model

Because of the very strong nature of the nucleon-nucleon interaction, it is assumed in this model that after a projectile enters the nucleus, it interacts very strongly with nucleons in the nucleus and the projectile loses its initial parameters and a new nuclear configuration, i.e. a combination of the projectile and the target nucleus (completely merged) is formed. From the conservation of energy, it is apparent that the compound nucleus will be formed at a highly excited state from which it has to decay to its own ground state by emitting gamma-rays or to another neighboring residual nucleus in the ground or excited state by emitting a particle.[10] In compound nucleus reactions the projectile is captured by the target nucleus and its energy is shared and re-shared among the nucleons of the compound nucleus until it reaches a state of statistical equilibrium.

The term compound nucleus reaction is commonly used for two different processes:

(i) capture of the projectile in the target nucleus to form a compound nucleus, which subsequently emits a particle or gamma,  
(ii) multiple emissions from the chain of excited residual nuclides following the binary reaction.[2,8,13] Information gained from the study of compound nucleus processes includes the properties of the states of the compound nucleus at energies just above the neutron binding energy which are excited in slow neutron capture, the mechanism of nuclear de-excitation including the role of the angular momentum and the nuclear deformation in affecting particle evaporation, and density of the high energy states.[8] Compound processes involve long reaction times ( $\sim 10^{-15}s$ ) and are predominant at low energies (below 10 MeV). In contrast with direct reactions, which are mostly one-step processes, the compound reaction mechanism is known to proceed by many intranuclear collisions.

The incident particle is captured by the target nucleus to form a compound nucleus. Subsequently, the incident energy is shared among the other nucleons and after a long time a sufficient amount of energy may be accumulated for one nucleon (or group of nucleons) to escape. Apart from conservation of total energy and total angular momentum,

the outgoing and incident channels are completely uncorrelated. These are reactions in which the incident particle interacts successively with a number of nucleons until most of its energy has been shared among many nucleons. In this extreme, the incident particle initiates a cascade of collisions. The first nucleon struck successively strikes others, and so on, until the randomness introduced by many collisions involving many nucleons causes loss of memory of what type of particle brought in the energy that is now shared throughout the nucleus. The compound nucleus has too much energy to be stable. However, because the energy of the projectile is now shared among many nucleons, it will survive for a relatively long time compared with the duration of a direct reaction.

Eventually, however, in the random course of events, one or more nucleons will acquire sufficient energy to escape. Low-energy neutrons are the most probable decay mode because, unlike charged particles, they experience no Coulomb barrier. The state in which the nucleus is left after this will probably be quite different from the ground state because of the fact that many nucleons shared the projectile energy. In fact, the randomness of the process suggests that one factor involved in predicting the energy of the residual nucleus is the level density in the residual nucleus. The other factor is the penetration factor or the probability that a particle of given energy can escape from the compound system. This is clearly an increasing function of decay energy. No single state will be strongly populated by the reaction because of the competition with other states, but the energy region populated will be at higher excitation where the energy levels are dense.[9] There is also a difference in the region of the nucleus where the two extremes dominate. Clearly, a peripheral collision (one in which the projectile passes through the diffuse surface of the nucleus) will most frequently lead to a simple collision, whereas when the projectile passes into the interior of the nucleus, it is more likely to suffer a number of collisions. We therefore expect that direct reactions are localized dominantly in the nuclear surface, whereas compound nuclear reactions are localized in the interior.[9]

### 2.2.3 The Optical Model

The interaction of a nucleon with a nucleus is inherently complicated and the optical model represents it by a phenomenological potential of very simple form, with parameters that are adjusted to fit the experimental data. This potential has an imaginary part that takes into account the absorption of the reaction flux from the elastic channel to the non elastic reaction channels. This is analogous to the scattering and absorption of light by a medium of complex refractive index, which is why it is called the optical model. Elastic scattering cross-sections are affected by the excited states of the compound system and by the residual states in the non-elastic channels. This causes the cross-section to fluctuate, and the fluctuations may be seen and analyzed when measurements of high precision are made on light nuclei. Optical potentials obtained by analysis of elastic scattering are widely used to generate the distorted waves used to analyze the cross-sections of many reactions, and these analyses have proved to be a powerful tool in determining nuclear structures. The optical model is basically mathematical model,[10] which replaces the physical nucleus by a potential, in which the scattering can be represented in terms of a complex potential  $u(r)$ :

$$u(r) = v(r) + iw(r) \quad (2.6)$$

Where the real functions  $v$  and  $w$  are selected to give the potential its proper radial dependence. The real part  $v(r)$  is responsible for the elastic scattering: it describes the ordinary nuclear interaction between target and projectile and may therefore be very similar to a shell model potential. The imaginary part,  $w(r)$ , is responsible for the absorption. We can demonstrate this by considering a square-well form for  $u(r)$ :

$$\begin{aligned} u(r) &= -v_0 - iw_0, r < R \\ &= 0, r > R \end{aligned} \quad (2.7)$$

The outgoing scattered wave we take to be in the form of  $e^{\frac{ik_r r}{r}}$ , with  $k = \sqrt{\frac{2m(E+V_0+iw_0)}{\hbar^2}}$ , which follows from solving the Schrodinger equation in the usual way for this potential. The wave number  $k$  is thus complex:

$$k = k_r + ik_i \quad (2.8)$$

Where,  $k_r$  and  $k_i$  are the real and imaginary parts respectively. The wave function behaves like  $e^{ik_r r} \cdot e^{\frac{-ik_i r}{r}}$ , and the radial probability density is proportional to  $e^{-2k_i r}$ . The wave is therefore exponentially attenuated as it passes through the nucleus.[2]

## 2.2.4 Pre-equilibrium or pre-compound Model

It can happen that a particle is emitted neither immediately after the interaction of the projectile with a nucleon or with a group of nucleons of the target nucleus, as in direct reaction, nor after a long time by the statistical decay of the compound nucleus. The projectile may share its energy among a small number of nucleons which may further interact with other nucleons, and during this cascade of nucleon-nucleon interactions through which the energy of the incident particle is progressively shared among the target nucleons, a particle may be emitted long before the attainment of statistical equilibrium. These processes are the pre-compound or pre-equilibrium reaction[8]. Hence the Pre-equilibrium reaction mechanism constitute the bridge between the fast, direct processes and slow, compound processes and provides an explanation for the observed high-energy tails in spectra and the smoothly forward peaked angular distributions. Nuclear reactions induced by  $\alpha$  particles at intermediate energy are characterized by pre-equilibrium (PE) particle emission followed by equilibrium (EQ) decay. As the projectile energy increases, the PE particle emission becomes more and more pronounced.

Hence the tail portion in the excitation function may not be explained unless the PE particle emission is taken into account.[14,15] For pre-equilibrium reactions involving deuterons up to  $\alpha$  particles, a (too low) contribution is automatically calculated within the exciton model reaction equations. However, for nuclear reactions involving projectiles and ejectiles with different particle numbers, mechanisms like stripping, pick-up and knock-out play an important role and these direct-like reactions need to be added incoherently.[13,16] The pre-equilibrium model has been traditionally aimed at study of reactions induced by particles with energies lower than 100 MeV.[17]

## Exciton Model

This model was proposed by Griffin in 1966 [8] for the formation and decay of the average compound nuclear state. The nuclear state is characterized by the excitation energy of the composite nucleus and the exciton number ( $n$ ), which is the total number of particles ( $p$ ) above and holes ( $h$ ) below the Fermi surface [18]. According to this model the interaction of a projectile with a target nucleus, gives rise to a simple initial configuration characterized by small number of excitons (excited particles and holes). Successive two body interactions increase the number of excitons and lead to a fully equilibrated residual nucleus. Griffin introduced two basic hypotheses to describe each stage of composite nucleus:

1. at each stage of the cascade all the states with the same configuration and the same total energy are equiprobable, and
2. at each stage of the cascade all the processes which may occur are also equiprobable.

The first hypothesis gives the energy distribution of the excitons. The second hypothesis simplifies the evaluation of transition rates obtained as suitable average over all the possible energies of the excitons in each configuration. In exciton model, any exciton creates a new particle-hole pair, exciton structure of the system is changed and it shifts to the next reaction stage. It takes into account the single pre-equilibrium emission in its standard formulation. Griffins model has widely been used and amplified by many authors. All the efforts put in the development and elaboration of this model made it a recognized and well established calculational mode for nuclear interactions. It is very useful to analyze the spectra of emitted particles and excitation functions of reactions up to hundreds of MeV energy. Many other semi-classical pre-equilibrium models have been proposed, most of them underestimate the experimental data. To overcome this deficiency, quantum mechanical models are formulated.

In the exciton and hybrid models, the nuclear state is characterized by the excitation energy  $E$  and the total number  $n$  of particles  $p$  above and holes  $h$  below the Fermi surface. Particles and holes are indiscriminately referred to as excitons. Furthermore, it is assumed that all possible ways of sharing the excitation energy between different particle-hole configurations with the same exciton number  $n$  have equal a-priori probability. To keep track of the evolution of the scattering process, one merely traces the temporal development of the exciton number, which changes in time as a result of intra-nuclear two-body collisions. This assumption makes the exciton model amenable for practical calculations. The price to be paid, however, is the introduction of a free parameter, viz. the average matrix element of the residual two-body interaction, occurring in the transition rates between two exciton states.

Restriction to two-body interactions leads to the following selection rules concerning the possible variation of the number of particles,  $p$ , holes,  $h$ , and excitons,  $n = p+h$ , in the course of the cascade of the interactions:

$$\begin{aligned}\Delta p &= 0, \pm 1 \\ \Delta h &= 0, \pm 1 \\ \Delta n &= 0, \pm 2\end{aligned}\tag{2.9}$$

After entering the target nucleus, the incident particle collides with one of the nucleons of the Fermi sea. Thus, an initial state with  $n_0 = 3$  is formed (in the case of nucleon-induced reactions). Subsequent interactions result in changes in the number of excitons, characterized by  $\Delta n = +2$  (a new particle-hole pair) or  $\Delta n = -2$  (annihilation of a particle-hole pair) or  $\Delta n = 0$  (creation of a different configuration with the same exciton number). In the first stage of the process, corresponding to low exciton numbers, the  $\Delta n = +2$  transitions are predominant.

However, at any stage there is a non-zero probability that a particle is emitted. Should this happen at an early stage, it is intuitively clear that the emitted particle retains some "memory" of the incident energy and direction: Bohrs amnesia hypothesis is not valid.

This phase is called the pre-equilibrium phase, which is expected to be responsible for the experimentally observed high-energy tails and forward-peaked angular distributions.

If emission does not occur at an early stage, the system eventually reaches a (quasi-) equilibrium. The equilibrium situation, corresponding to high exciton numbers, is established after a large number of interactions, i.e. after a long lapse of time, and the system has "forgotten" about the initial state. Accordingly, this stage may be called the compound or evaporation stage. Hence, in principle the exciton model enables to compute the emission cross sections in a unified way, without introducing arbitrary adjustments between equilibrium and pre-equilibrium contributions. The equilibration process is most completely described quantitatively by the master equation exciton model. The other types of exciton and hybrid models may be considered simplifications or variants of this model. The master-equation model, which predicts energy distributions of emitted particles, is discussed in the next subsection.

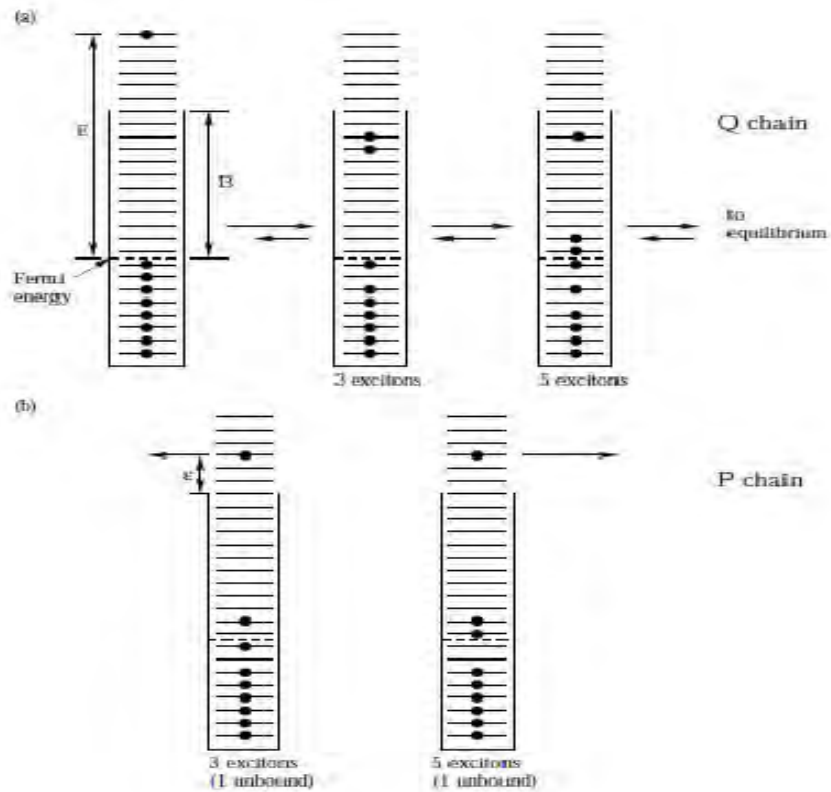


Fig.(2.5). A schematical representation of the first few stages of a nucleon-induced

reaction in the exciton model and Feshbach, Kerman and Koonin (FKK) theory. The horizontal lines indicate equally spaced single-particle states in the potential well. The particles are shown as solid circles.  $E$  is the particle energy measured from the Fermi energy and coincides with the initial excitation energy;  $B$  is the average binding energy. Part (a) shows nucleon-nucleon interactions leading to more complex configurations in which all particles are bound and thus cannot be emitted. In FKK theory this sequence of processes is called the Q chain. Part (b) shows interaction leading to configurations in which at least one particle is unbound and thus may be emitted into the continuum with energy  $\varepsilon$  leaving a residue with energy  $U = E - B - \varepsilon$ . In FKK theory this sequence of processes is called the P chain. The exciton model does not make any distinction between the two types of process.[ 8]

**The master equation exciton model:** The pre-equilibrium master equation was first proposed by Cline and Blann. Let  $q(n, t)$  be the probability that the nuclear system is in the exciton state  $n$  at time  $t$ . For notational simplicity, we do not indicate the dependence of the excitation energy. Also, we note in advance that in subsequent years the master equation has been generalized to include a dependence on angle (generalized exciton model), angular momentum, parity and isospin. The time evolution of the exciton probability distribution is given by the master equation:

$$\begin{aligned} \frac{dq(n, t)}{dt} = & \lambda^+(n-2)q(n-2, t) + \lambda^-(n+2)q(n+2, t) \\ & - [\lambda^+(n) + \lambda^-(n) + w(n)]q(n, t) \end{aligned} \quad (2.10)$$

Here,  $\lambda^+(n)$  and  $\lambda^-(n)$  are the internal transition rates from state  $n$  with  $\Delta n = +2$  and  $\Delta n = -2$  respectively, whereas  $w(n)$  indicates the total emission rate from state  $n$  summed over all outgoing particles and energies[10];

$$w(n) = \int d\varepsilon \lambda_c^n(\varepsilon) \quad (2.11)$$

Eq. (2.10) is a gain-loss equation, the positive terms representing the feeding to a particular state  $n$  and the negative terms describing the loss to other states. The term with  $w$  is a sink term describing the decay of the nucleus. To solve Eq. (2.10) it should be supplemented by an initial condition. For nucleon-induced reactions the most obvious choice

is;  $q_0(n) \equiv q(n, t) = 0 = \delta n, n_0$  with  $n_0 = 3$ . We note that in Eq.(2.10) the transitions with  $\Delta n = 0$ , having transitions rates  $\lambda^0(n)$ , cancel and therefore do not contribute. In the generalized exciton model, where angular distributions are taken into account,  $\lambda^0(n)$  does play a role.[8,19]

## 2.2.5 Other semi-classical models

### The Harp-Miller-Berne (HMB) model

The Harp-Miller-Berne (HMB) model [10] was proposed before the exciton model by Griffin, divided the phase space of particles below Fermi energy into groups or bins, whose  $\Delta E$  is chosen to be of some convenient dimension. This is in contrast to the exciton model, where all energy partition between particles and holes in a given exciton state occur with equal probability. In HMB model, one calculates the occupation probability of an average state in the  $i$ th bin as a function of time. At time  $\tau = \tau_0$  all the particles and levels are below the Fermi-energy and the incident particle is in the excited state giving certain group occupation probability. Two-body interactions then, lead to re-distribution of probabilities. The following Master equation for a single particle gas of nucleons applies on HMB model:

$$\begin{aligned} \frac{d}{dt}(n_i g_i) &= \sum_{j,k,l} \omega_{kl,ij} g_k n_k g_l n_l (1 - n_i)(1 - n_j) g_i g_j \\ &- \sum_{j,k,l} \omega_{ij,kl} g_i n_i g_j n_j (1 - n_k)(1 - n_l) g_k g_l - n_i g_i \lambda_c(i') \end{aligned} \quad (2.12)$$

Where  $i'$  is the energy outside the nucleus corresponding to the  $i$ th bin in the nucleus. Physically this equation gives the net rate of change of number of nucleons in the  $i$ th bin with  $g_i$  as the number of single particle states/MeV in one MeV bin-width for  $\Delta E$  and  $n_i$  as the number of particles in each state. The first term on the right represents the increase of particles in bin  $i$  from the inter-nucleon N-N scattering process, the second term on the right as loss due to the same process and the third term as loss of particles from  $i$  due to emission into the continuum where  $\lambda_c(i')$  is the emission rate into the continuum of a particle.  $\omega_{kl,ij}$  represents the transition rate for a nucleon in one of the state  $i$  to collide with one in state  $j$ , such that two nucleons go to the energy conserving state  $k, l$ .

The quantity  $n_i g_i$  or  $g_j n_j$ , etc. gives the number of nucleons in the  $i$ th or  $j$ th energy interval with  $g_i$  or  $g_j$  as single particle state/MeV.  $\omega_{ij,kl}$  again represents the transition probability of corresponding states.

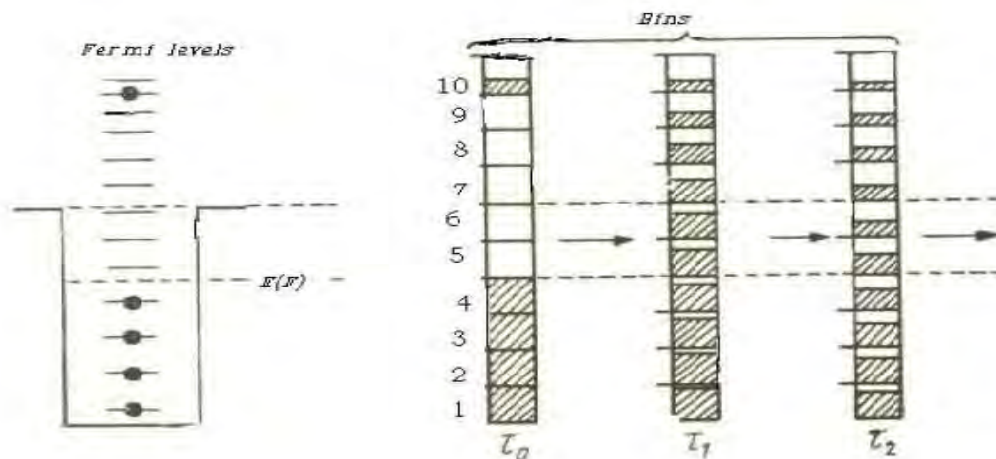


Fig.(2.6) Illustration of equilibrium process as formulated by the master equation of HMB model. The shaded areas represent the occupied fraction of each bin with occupation changing after each time interval.[3]

### The Hybrid Model

This model combines HMB model and exciton model in such a manner that, while the basic scenario of the evolution of the reaction process inside the nucleus follows the exciton procedure, the counting of levels is done, by using HMB model. The hybrid model describes the  $n$ -exciton state as made of two systems, a real system corresponding to the residual nucleus with exciton number  $n-1$ , but with excitation energy  $U$ , [ $U=E-(B+\varepsilon)$ ] characterised by the level density  $\rho_{n-1}(U)$  and a virtual system of nucleons, in an unbound state characterized by the single particle level density,  $g$ . Each unbound particle will have  $g d\varepsilon$  levels available to it between energies  $\varepsilon$  and  $\varepsilon+d\varepsilon$ . For each of these levels, the level density is  $\rho_{n-1}(U)$ . Hence the total level density available to the outgoing particles is  $\rho_{n-1}(U)d\varepsilon$ . [10]

## 2.2.6 Interanuclear Cascade Model

The interanuclear Cascade model has been traditionally aimed at study of reactions induced by particles with energies higher than 100 MeV.[10,17] However, it has been recently used for lower energies for explaining the pre-equilibrium spectra. The trajectory of an excited particle is followed until it reaches the nuclear surface or its energy goes below a certain level governed by Pauli Exclusion Principle. Every particle which reaches the surface above a certain energy required to cross the surface is assumed to belong to an emitted particle. Then one starts with another impact parameter and goes through the same calculations till one covers all the values of impact parameters. This gives the cross section of the emitted particles of different emitted energies and their angles.[10]

## 2.2.7 Heavy ion reactions

Heavy ion induced reactions are usually taken as reactions induced by projectiles heavier than an alpha particle.[1] The span of projectiles studied is large, ranging from the light ions, C, O, Ne to the medium mass ions, such as S, Ar, Ca, Kr to the heavy projectiles, Xe, Au and even U. In the light-nucleus region we have assumed that the neutron and proton are “isotopically” similar; in the heavy-nucleus region, in which an important role is played by Coulomb forces, this assumption is no longer valid. Whereas the properties of light nuclei depend on the total number of nucleons in a shell, the properties of heavy nuclei depend on the number of neutrons, N, and the number of protons, Z, individually. Accelerators devoted to the study of heavy-ion reactions can produce beams of ions up to  $^{238}\text{U}$ , at typical energies of the order of 1-10 MeV per nucleon, although much higher energies are also possible.[2] Reactions induced by heavy ions have certain unique characteristics that distinguish them from other reactions. The wave length of a heavy ion at energy of 5MeV/nucleon or more is small compared to the dimensions of the ion. As a result, the interactions of the ions can be described classically. The value of the angular momentum in the collisions is relatively large. For example we can write:

$$l_{max} = \frac{R}{l} \left(1 - \frac{B}{\varepsilon}\right)^{1/2} \quad (2.13)$$

The heavy ion induced reactions are somewhat complex because of the complexity of the incident projectile. Because of the heavy mass of the incident heavy ion, a lot of energy and angular momentum can be imparted to the target nucleus giving rise to new phenomenon, e.g. fusion-fission, etc. Heavy ion reactions basically differ from the light ion induced interactions in the fact that the heavy ion projectiles have a large number of nucleons in it and hence when a projectile enters the nucleus; there is a diffusion of nucleons to the projectile from the nucleus and from the projectile to the nucleus. The modified HMB master equation describing the heavy ion reaction for a one- Fermi-ion gas type gas in the projectile and target nuclei is written as:[10]

$$\begin{aligned} \frac{d(n_i g_i)}{dt} = & \sum_{j,k,l} \omega_{kl,ij} g_k n_k g_l n_l (1 - n_j) g_i g_j \\ & - \sum_{j,k,l} \omega_{ij,kl} g_i n_i g_j n_j (1 - n_k) (1 - n_l) g_k g_l - n_i g_i \omega_{ii'} g_{i'} + \frac{d}{dt} (n_i g_i)_{fusion} \end{aligned} \quad (2.14)$$

Where  $n_i$  = average occupation number for the  $i$ th bin above the bottom of nuclear well, each bin being of 1MeV interval,

$g_i$  = number of single particle states per MeV in an energy introduced around  $i$ th bin.

$\omega_{ab,cd}$  = the transition probabilities for nucleons in initial state  $a$  and  $b$  to scatter into final states  $c$  and  $d$ . These are evaluated from free nucleon-nucleon scattering cross section.

The fractional occupation members  $g_j(1-n_j)$  etc. which multiply the free nucleon-nucleon collision rates give Pauli-Exclusion correction;  $\omega_{ii'}$  gives the rate, for particle at energy  $i$  within the nucleus to go to energy  $i'$ , outside the nucleus (continuum). The first two terms in eq. (2.14) give the rates of scattering particles into and out of the interval  $i$  by two body collisions and the third term gives the rate of emission into continuum. The fourth term represents a time dependent addition to nucleons to the equilibrating system (Coalescing system) from the projectile.

# Chapter 3

## Computer Code COMPLET

The code COMPLET is a nuclear reactions code which was designed for versatility and ease of use in the bombarding energy range of a few MeV to several hundred MeV. The code COMPLET is based on same philosophy as the former code COMPLEX and an extension of code INDEX.[20] COMPLET code is an extension of the code ALICE-91 and INDEX. These two codes employ the Weisskopf-Ewing model for the statistical part and geometry dependent hybrid model of M.Blann for the pre-equilibrium emission. The code COMPLET gives the result of compound reaction and compound nucleus plus pre-equilibrium reaction. The projectile energy is measured in Mega Electronvolt (MeV) and the cross-section are measured in millibarn(mb).

In COMPLET code a pre-equilibrium process in two stages is assumed. The particles in the initial configuration ( $n_0 = EX1 + EX2 + EX3$ ) can be neutron, proton or alpha particle, represented by the exciton numbers EX1, EX2 and EX3 respectively. It is customary to use the initial exciton number  $n_0$  separated in to proton and neutron above and holes below the Fermi level as a fit parameter to match theoretical prediction with experimental excitation function. The requirement of detailed input parameters was sacrificed to achieve this goal.

The code COMPLET provides yields and spectra for all reactions populated by all combinations of  $n, p, d, \alpha$  and can provide all input parameters internally. The running time of the code is very short. This code includes damping of fission widths above a critical temperature  $R_0$ . The used code is a further simplification of the formulae due to Paul

and Thoennessen in Ann.Rev.Nucl and particle science 44(1944). The code COMPLET includes pre-equilibrium neutron, proton and alpha emission up to two particle, as well as evaporation of neutrons, protons, alphas, deuterons, tritons and hellions.

Originally, this code has been developed out of the code OVERLAID ALICE by M.Blann, while some standard routines remained practically unchanged (like FISROT, LYMASS, PUNCH, PLT, PARAP, OVER1, OVER2 and TLJ) others have been substantially modified (like MAIN, SHAFT, NUCMFP, etc) or are completely new (like, INDEX, PARDEN, TRAPRO, ANGULAR, etc) the underlying PE-MODEL is described in Z.Phys.A328 (1989).It is contained in subroutine INDEX.

The INPUT is described below. The notion card from the old FORTRAN input is still kept but now corresponds to lines. Free formats, the input values should be separated by ",," or CR".

#### CARD 1 - GENERAL INPUT DATA

AP	Projectile mass number		
AT	Target mass number		
ZP	Projectile charge		
ZT	Target charge		
QVAL	Reaction $Qvalue = AP + AT - ACN$		
		= 0: calculated from M and S mass formula.	
		= 1: calculated from mass excesses of 1990 nuclear wallet cards	
PLD	Level Density Parameter $a$ , $a = CAN/PLD$ .	= 0:	$a = CAN/8$
CLD	Ratio of single particle level densities $AF/AN = 0$ :		$AF/AN = 1.0$
BARFAC	Multiplies the rotating drop fission barrier by this value.	= 0:	$BARFAC = 1$
ROTFAC	Multiplies the rotational energy by this value.	= 0 :	$ROTFAC = 1$ .
RO	Critical temperature above onset of retarded fission		
GI	Nuclear friction parameter from equilibrium deformation to saddle		
GO	Nuclear friction parameter from saddle to scission point		

NA Number of nuclides of each Z to be included in calculation. Up to 21 neutrons may be emitted (Maximum NA=22)

NZ Number of Z- values to be calculated in the emission process. Up to 8 protons may be emitted (Maximum NZ=9).

For correct PE calculations binding energies are calculated for all nuclei with  $IZ, IA \leq 5$

MC Shell correction option for masses subroutine.  
= 0, Shell correction.  
= 1, No shell correction  
= 2, BE values will be supplied as input.  
>2, BE values are calculated from 1990 nuclear wallet cards.

MP Pairing correction to masses.  
= 0: No correction  
= 1: pairing term  
=2: masses are from nuclear wallet cards;  
=3: pairing correction in masses, NOTE: changes are not corrections in only level densities

IPA Pairing corrections in level densities  
IP= -1, No corrections  
IP =0, standard correction i.e multiplier =12  
If IPA>0 multiplier is IPA

M3 Number and type of particles to be emitted from each nuclide  
If = 1: N only;= 2:N and P;=3 or =0:N,P and Alpha;=4:N,P,Alpha and Deuteron = 5:  
N, P, Alpha, Deuteron and Triton;=6: N,P, Alpha, Deuteron, Triton and hellion (3He);  
=7: as before includes Gammas.Calculations until gamma emission is finished, important for isomeric ratio calculations.

INVER Inverse cross section parameter = 0: user will supply; =1: results by O.M subroutines as ALICE/85/300,

If = 2 O.M for N, p as in old ALICE; If =3: sharp cutoff values for inverse cross sections.

IKE If = 1 No particle spectra will be printed;

If= 2 Equilibrium spectra for each nuclide will be printed;

If =3: Only pre-compound spectra will be printed;

If = 5: PE and summed equilibrium spectra will be (separately) printed;

If =4 AS 2+3

If IKE = -2 to -5: reduced output with spectra as  $IKE = ABS(IKE)$  (yields are printed after negative energy input)

If  $IKE \leq 0$  or  $IKE = 6$  most reduced output

IPCH = 1: inverse cross sections will be readout for possible future use in separate output file.

= 0: or NE from 1, No printout

KPLT Number of decades to be plotted as excitation function on line printer.

If KPLT = 0: no plotting

## **CARD 2 TITLE CARD**

If MC = 2 on CARD 1, read user supplied n, p, alpha, deuteron, triton and helion binding energies here, Format for IA =1 to NA, IZ=1 to NZ. If INVER =0 on CARD1, read n, p, alpha, deuteron, triton, helion and gamma inverse cross sections here. In ascending channel energy, first value = 0.1 MeV, incremented by 1MeV, 48 values per particle type in sequence N,P,A,D,T,3HE, and Gamma depending on value of M3.

## **CARD 3 ENERGY and CN&PE OPTIONS**

IKEN projectile kinetic energy in the laboratory system.

If = 0: A new problem will begin at CARD1.

If < 0: previously calculated excitation functions will be printed (if not KPLT=0, EKIN values were run in ascending order they are plotted). If EKIN=0 on two successive cards, a normal exit will occur for negative target mass on card 1.

RCSS = 0: Reaction cross section is calculated from subroutine (for pi-induced reactions: if RCSS (input) =0, RCSS=100 mb) if input > 0: number of T(1) values to be read from the next card

JCAL Tyoes of calculation options

= 1, weisskopf-ewing evaporation calculation,

= 2, S- wave approximation, liquid drop moment of inertia,  
 = 3, S- wave with rigid body,  
 = 0, Calculation for all partial wave including fission and full angular momentum coupling up to DELTA L=12.

JFRAC        Direct- semidirect capture gamma ray estimate :<0: no emission,> 0: approach of kalka, =0 simple approach with initial exciton-number = 1 for P,N.

JANG        JANG + 1 = maximum number of contributing incoming partial waves.  
 Usually use the maximum: JANG =99. Otherwise, JANG can be used for cutoff on L-values provided by subroutines OVER1 and 2

All additional parameters on this card are for the pre-compound calculation options. Put TD-values to zero, if no pre-compound calculation is wanted.

TD        Initial exciton number =p+h

EX1        Initial excited neutron number

EX2        Initial excited proton number

EX3        Initial alpha particle exciton number

POT        Fermi energy in Mev

If = 0: POT is calculate from nucl.matter value= 37.8 Mev;

AV        If = 0: OPTICAL MODEL mean free paths are used in routine MFP.  
           Not to be used above 55 Mev.

If AV = 1: Nucleon-Nucleon mean free paths are used in NUCMFP.

ALF        Probability that newly created exciton particle from first stage exciton gets an alpha particle in the second stage.

(1-ALF): complementary probability

If ALF>1 calculation for two initial exciton numbers

A) ATD=TD-3 (min.1.5) AEX1=AEX2=0. AEX3=2;ATD=TD-6 for TD>9

with weight ULF=INT (ALF)100

B)Weight = (1-ULF), with initial exciton numbers.

CMFP        Mean Free Paths are multiplied by CMFP.if CMFP =0:multipplier is 1

GDO        Critical angular momentum.

GDO>0: partial waves with  $L > GDO$  are not taken in to account in the (second) line of isotone cross sections while cross sections for partial waves with  $L > GDO$  are accounted for in the (third) line below N.B For  $GDO \leq +0.5$  No cut-off.

**CARD 4 ENERGY AND REACTION CROSS SECTION**

EKIN Projectile kinetic energy in the laboratory system

This card is repeated for each energy wanted in calculating excitation function with parameters specified in card 1 and card 3.

RCSS As on card 3

**CARD 5 ISOBARIC YIELD CALCULATIONS IN EXCITATION FUNCTIONS**

(Card 5 is read after negative energy on card 4 or 3)

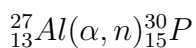
ISOBA 28 numbers are expected since maximum 28 isobaric chains exist starting from CAN-1. The 28 ISOBA inputs may vary from 0 to 9 according to the number of ISOBARS to be added.

# Chapter 4

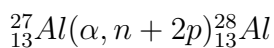
## Reaction Channels, Analysis and Discussion

### 4.1 Reaction Channels

#### 4.1.1 Reaction Channels of $^{27}\text{Al}$



This reaction obtained by evaporation of one neutron from the composite nucleus. The residue is a radioactive nucleus,  $^{30}\text{P}$ , is unstable and further decay to  $^{30}\text{Si}$  by the decay mode of electron capture. The half life of  $^{30}\text{P}$  is  $T_{1/2} = 2.5\text{min.}$  and its spin is  $1^+$ .



The residue nucleus  $^{28}\text{Al}$  is the result of the evaporation of three nucleons (one neutron and two protons) from the composite nucleus. The residue nucleus is unstable and decay to  $^{28}\text{Si}$  (Stable) having the half life time  $T_{1/2}=2.24\text{min.}$  undergoes the decay mode of  $\beta^-$  emission. Its spin is  $3^+$ .

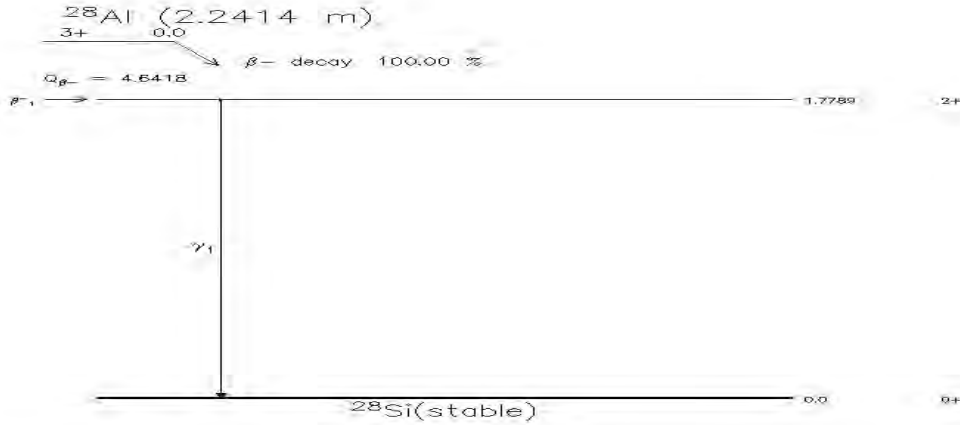
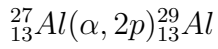
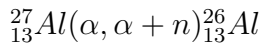


Fig. 4.1 Decay Scheme of  $^{28}\text{Al}$



The reaction channel results in the evaporation of two protons from the compound nucleus forming the residue nucleus  $^{29}\text{Al}$ . This residue nucleus is unstable and further decays to  $^{29}\text{Si}$  through  $\beta^-$  emission decay mode. Its half life and spin is 6.56min and  $5/2^+$  respectively.



This channel is characterized by the emission of five nucleons (a  $^4\text{He}$  nucleus and one neutron). The residual of the evaporation can be the metastable  $^{26m}\text{Al}$  nucleus with a very short life time, ( $T_{1/2} = 6.35\text{s}$ ) and spin of  $0^+$  and  $^{26}\text{Al}$ .  $^{26}\text{Al}$  is a radioactive isotope with a life time of 0.72 million years. During the decay to the stable isotope,  $^{26}\text{Mg}$ , it emits almost always a 1.8086 MeV gamma ray photon, in roughly 85% of the decays. The disintegration of  $^{26}\text{Al}$  is also accompanied by the emission of a positron. Eventually, this positron will encounter electrons of the environment, and annihilate under the emission of 2 photons of 511 keV or 3 photons with energies below 511 keV. Additional gamma ray lines occur during the decay of  $^{26}\text{Al}$  at 1.1297 MeV (2%) and 2.938 MeV (0.2%). The following figure illustrates the decay scheme of  $^{26}\text{Al}$ .

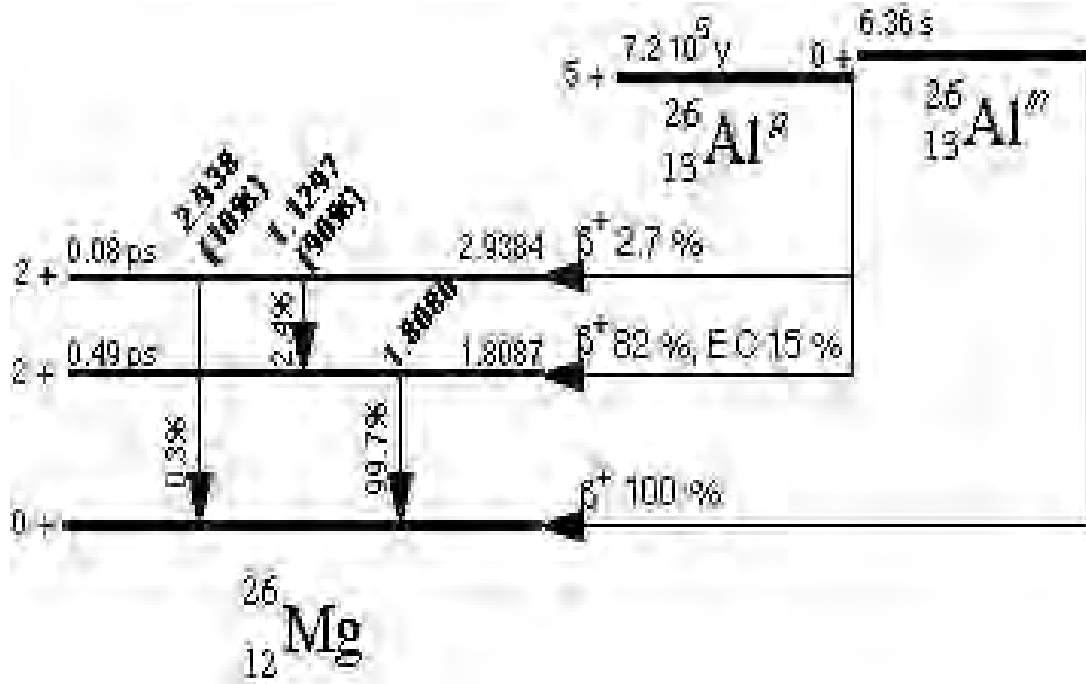
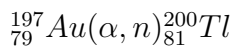


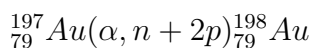
Fig. 4.2 Decay Scheme of  $^{26}\text{Al}$

#### 4.1.2 Reaction Channels of $^{197}\text{Au}$

Gold ( $^{197}\text{Au}$ ) is the most naturally occurring stable isotope. However, by inducing energetic projectiles it is possible to produce unstable nuclei. For comparison reason similar reaction channels with the previous section were taken and analyzed.



The reaction takes place by the evaporation of one neutron from the compound nucleus. The residue of the evaporation,  $^{200}\text{Tl}$  nucleus, is unstable which decays to  $^{200}\text{Hg}$  through the process of positron emission. The residue nucleus has a half life of 26.1hrs and the spin of  $2^-$ .



The emission of three nucleons (one neutron and two protons) comes out from the composite nucleus by remaining the residue metastable nucleus,  $^{198m}\text{Au}$  and the excited  $^{198}\text{Au}$  nucleus. The metastable has a half life of 2.27 days and undergoes the decay mode of

isomeric transition. It also has spin parity of  $12^-$ . The excited residue nucleus,  $^{198}\text{Au}$  has a life time of 2.7 days and spin parity of  $2^-$ . A somewhat more complicated scheme is shown here: the decay of the nuclide,  $^{198}\text{Au}$ , which can be produced by irradiating natural gold in a nuclear reactor.  $^{198}\text{Au}$  decays via  $\beta^-$  decay to one of two excited states or to the ground state of the mercury isotope  $^{198}\text{Hg}$ . In the figure, mercury is to the right of gold, since the atomic number of gold is 79, that of mercury is 80. The excited states decay after very short times (2.5 and 23 ps, respectively) to the ground state.

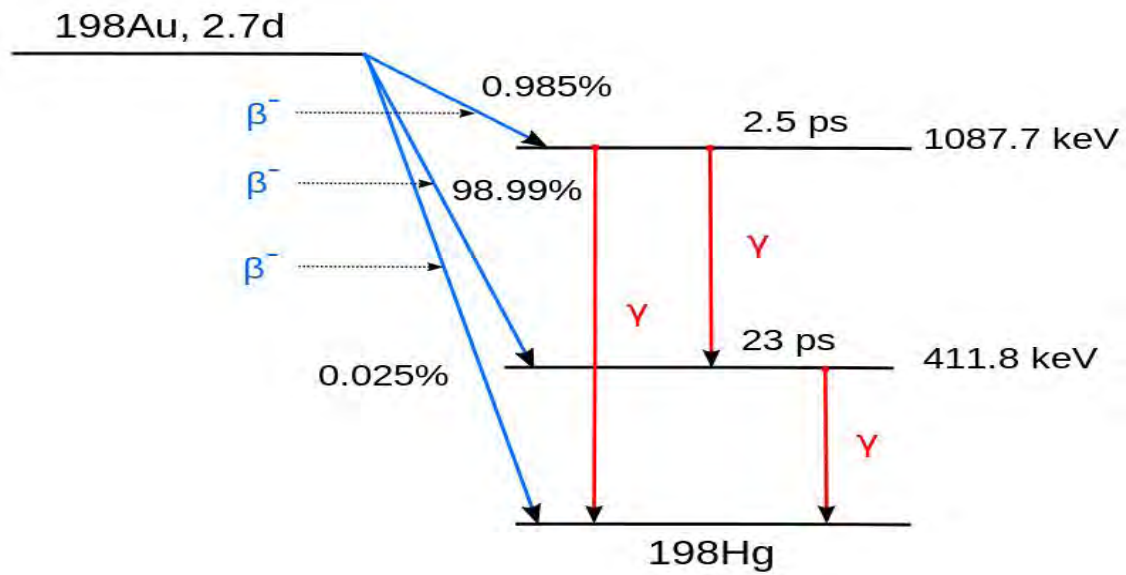
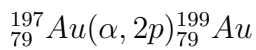


Fig. 4.3 Decay scheme of  $^{198}\text{Au}$



The evaporation of two protons from the composite nucleus results in the residue of  $^{199}\text{Au}$  nucleus which is unstable and decay to  $^{199}\text{Hg}$  (stable) by mode of  $\beta^-$  emission. Its spin parity is  $3/2^+$  and half life is 3.14 days.

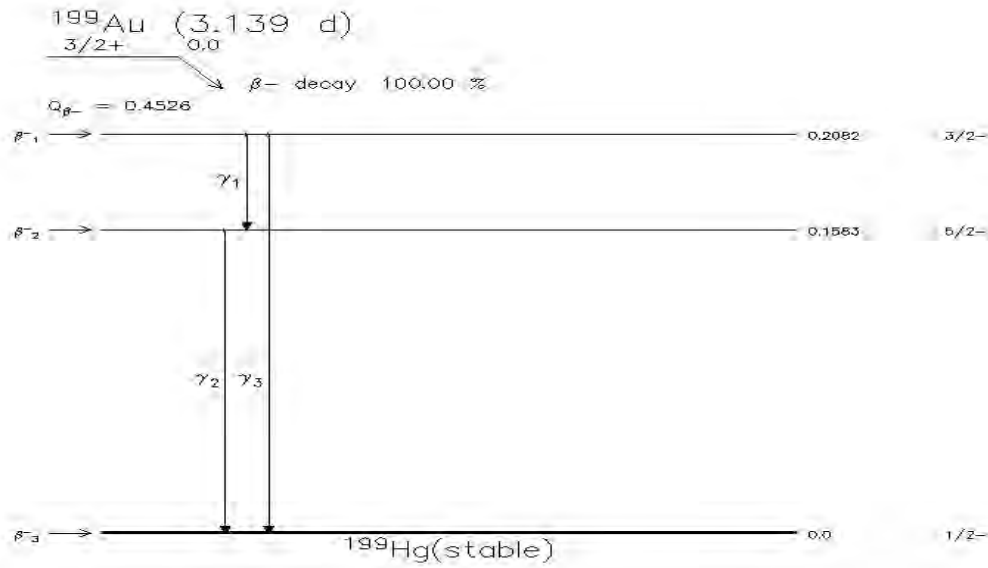
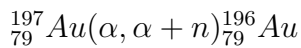


Fig. 4.4 Decay scheme of  $^{199}\text{Au}$



The reaction channel results in the emission of five nucleons (one neutron and a  $^4\text{He}$  nucleus) from the composite nucleus. The evaporation residue is a radioactive nucleus,  $^{196}\text{Au}$ . It has a spin parity of  $2^-$  and half life of 6.183days. It decays to  $^{196}\text{Hg}$  (stable) by the mode of Electronic capture (92.8%) and  $\beta^-$  emission (7.2%).

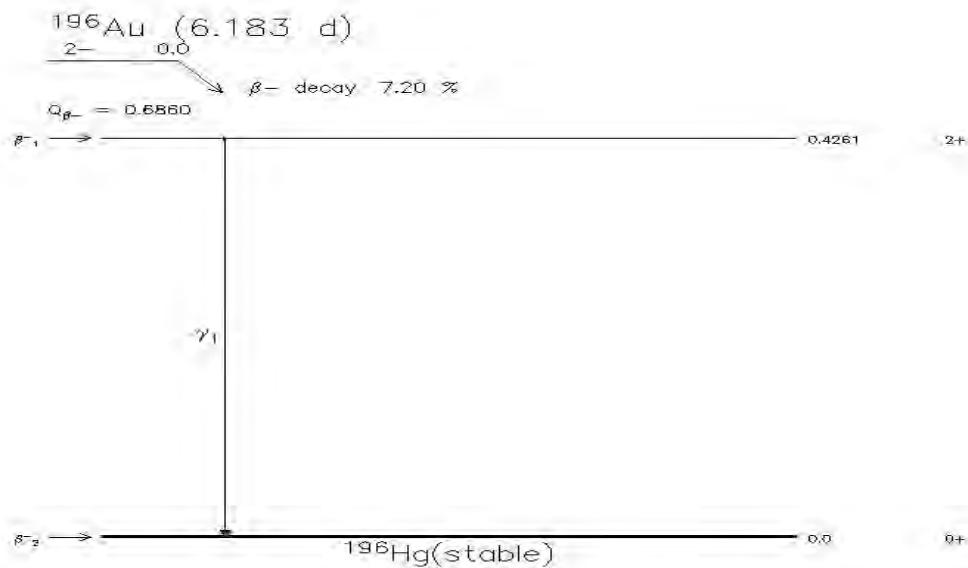


Fig. 4.5 The decay scheme of  $^{196}\text{Au}$

## 4.2 Analysis and Discussion

This chapter presents sample description and characterization, describes and summarizes the main results, which are discussions of the main trends, patterns and connections that have emerged which is preceded by tables and plots. The excitation function of alpha-particle induced reaction on the isotopes of  $^{27}\text{Al}$  and  $^{197}\text{Au}$  are theoretically evaluated using computer code COMPLET. The Experimental cross-section is obtained from IAEA data source, EXFOR Library.[3] The theoretical and experimental cross-sections are plotted against the projectile energy and are shown in fig. 4.6 to fig. 4.13.

The theoretical calculation is performed for two cases. These are for pre-equilibrium plus compound nucleus decay excitation function and for only compound nucleus decay excitation function. The excitation function for pre-equilibrium plus compound reaction is shown by the blue color, compound reaction is shown by green color and the excitation functions for the experimental results with errors are shown by the red color.

The excitation function produced by the target of light nucleus,  $^{27}\text{Al}$ , and heavy nucleus,  $^{197}\text{Au}$ , with similar reaction channel was compared and explained against each other. Energy range selected from the experimental data from EXFORE is same with theoretical. The cross-section of theoretical and experimental with the selected energy range are given in tables 4.1 to 4.8.

The various parameters are used for calculations of excitation functions. However, the initial exciton number is found to play an important role in the theoretical predictions for pre-equilibrium reactions. In this thesis the initial exciton number ( $n_0 = 4$ ) with configurations (2p+2n+0h) has been mainly taken for  $\alpha$  projectile, which interact independently with particles below the Fermi level creating either new particle-hole configuration in the second stage or getting emitted in to the continuum. However, the initial exciton number ( $n_0 = 6$ ) with configurations (3p+2n+1h) has been taken for  $\alpha$  projectile in the reaction channels of  $^{27}_{13}\text{Al}(\alpha, 2p)^{29}_{13}\text{Al}$  and  $^{197}_{79}\text{Au}(\alpha, 2p)^{199}_{79}\text{Au}$ . This occurred because of significant difference between the experimental and theoretical plots where initial exciton number

( $n_0 = 4$ ) is employed for these particular reaction channels.

Level density parameter also plays an important role in calculating the nuclear reaction model statistically, such as in calculating the evaporation model of nuclear reaction and in studies of intermediate-energy of heavy ion collision [21]. The level density parameter obtained by experiment shows a linear dependent with the mass number of the compound nucleus. In general it is given by an expression,

$$a = \frac{ACN}{K} \quad (4.1)$$

where ACN is the mass of the compound nucleus and K is the free constant. In this thesis the level density parameter  $a = \frac{ACN}{8}$ ,  $a = \frac{ACN}{9}$  and  $a = \frac{ACN}{10}$  were employed for respective reactions, which gives the best fit to experimental results. The cause for the variation of the value of K here is that seeking for the best fit to the experimentally measured excitation function. However, effort had been made to use the same K value for analogous reaction channels of the two isotopes for reasonable comparison. The nuclear level density  $\rho(E)$  is a characteristic property of every nucleus and it is defined as the number of levels per unit energy at a certain excitation energy. Average level density:

$$\rho(E) = \frac{dN}{dE} \quad (4.2)$$

In other words it is the number of different ways in which individual nucleons can be placed in the various single particle orbital such that the excitation energy lies in the range E to E+dE. It increases rapidly with excitation energy. In the simplest approach, the nucleus can be considered as a system of fermions which can occupy levels equidistant in energy. The density of excited states is given as [22]

$$\rho(E) = \frac{\exp(2\sqrt{aE})}{4\sqrt{3E}} \quad (4.3)$$

Where the parameter  $a$  is known as the level density parameter. A more realistic extension of this model considers the fact that fermions have the tendency to form pairs, and that it takes an extra amount of energy to separate them. This can be taken into account by introducing a shift E in the excitation energy (E is considered as an adjustable parameter), which leads to the Back - Shifted Fermi Gas model (BSFG) [22].

#### 4.2.1 $^{27}_{13}\text{Al}(\alpha, n)^{30}_{15}\text{P}$ Reaction

Projectile			
Energy(MeV)	$\sigma(\text{exp.})(\text{mb})$	$\sigma(\text{Com.})(\text{mb})$	$\sigma(\text{Com.} + \text{Pre-com.})(\text{mb})$
10	-	296.7	294.5
10.5	50	-	-
13.8	340	-	-
15	400	401.1	389
16	280	-	-
18.1	163	-	-
20	105	415.5	390
21	86	-	-
22	81	-	-
23	45	-	-
25	-	294.6	247.6
27.6	21	-	-
30	-	235.3	190.5
35	-	166.6	124.8

Table: 4.1. Theoretical and Measured Cross-Section for the Reaction  $^{27}_{13}\text{Al}(\alpha, n)^{30}_{15}\text{P}$

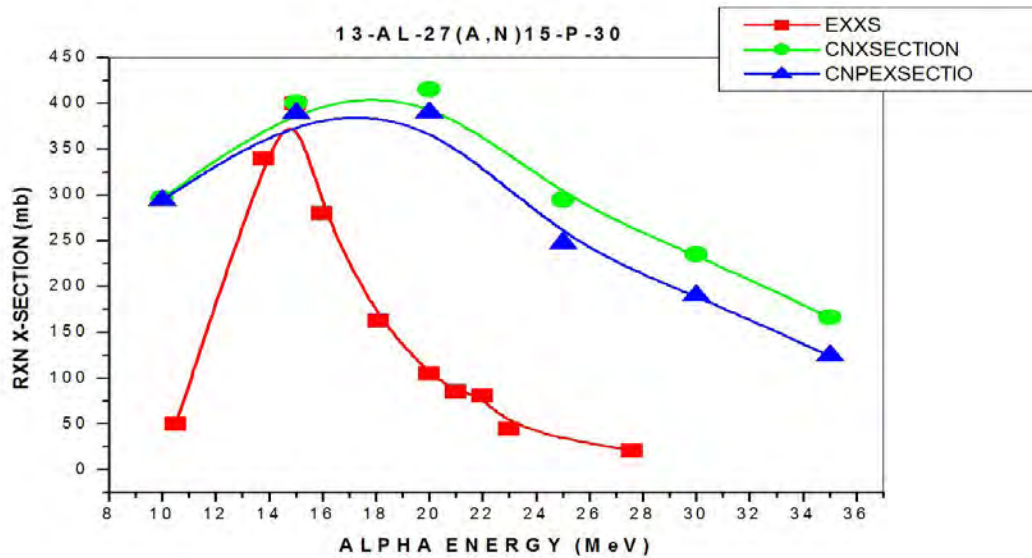
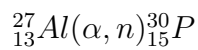


Fig. 4.6 Experimental and Theoretical Excitation Function for the Reaction



The results presented in table (4.1) and fig. (4.6) shows that the experimental values of excitation function in the reaction shows a peak around 15 MeV While in the calculated values both the compound nucleus theory and pre-compound theory gives a broad peak around 19 MeV.

The experimental value of the excitation function falls very rapidly and around 28 MeV it is about 1/10 of the theoretical value. Theoretical values do not fit with the experimental results. Thus the reaction can be explained neither by the compound nucleus reaction model nor by the pre-equilibrium model, but could be direct stripping reaction.

#### 4.2.2 $^{197}_{79}\text{Au}(\alpha, n)^{200}_{81}\text{Tl}$ Reaction

Projectile				
Energy(MeV)	$\sigma(\text{exp.})(\text{mb})$	Error(mb)	$\sigma(\text{Com.})(\text{mb})$	$\sigma(\text{Com.} + \text{Pre} - \text{com.})(\text{mb})$
10	-	-	0	0
10.4	0.8	0.9	-	-
13.8	1.3	0.8	-	-
15	-	-	0.1832	0.1832
16.9	5.7	1.6	-	-
19.4	15.7	4.0	-	-
20	-	-	7.379	12.04
22.9	17.2	4.3	-	-
25	-	-	0.6169	19.88
26.1	11.9	3.0	-	-
29	6.9	1.8	-	-
30	-	-	0.05461	26.3
33.5	5.4	1.3	-	-
35	-	-	0.00161	21.42

Table: 4.2 Theoretical and Measured Cross-Section for the Reaction  $^{197}_{79}\text{Au}(\alpha, n)^{200}_{81}\text{Tl}$

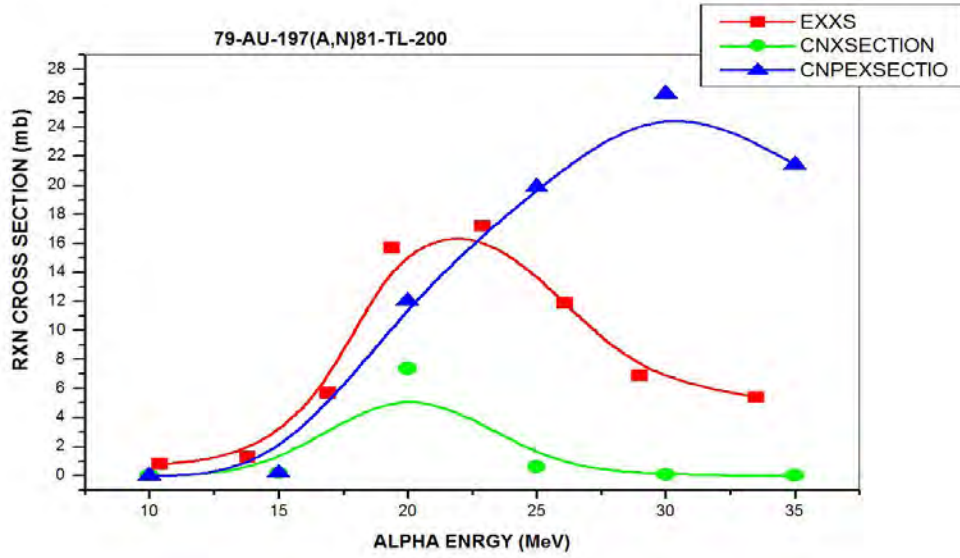


Fig. 4.7 Experimental and Theoretical Excitation Function for the Reaction

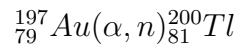


Table (4.2) and fig. (4.7) show when alpha particle is bombarded on target of heavy nucleus ( ${}^{197}\text{Au}$ ). The nature of the reaction depends on the energy of the projectile. From the graph we can see that for the lower energy (about  $<13\text{MeV}$ ) both the theoretically calculated pre-equilibrium and the compound nuclear reactions seems overlap. However the compound nuclear reaction dominates the reaction in such lower energy range. In the higher energy region the graph of theoretically calculated pre-equilibrium excitation function approaching the result of the experimental value obtained from the data source.

### 4.2.3 $^{27}_{13}\text{Al}(\alpha, n + 2p)^{28}_{13}\text{Al}$ Reaction

Projectile	Energy(MeV)	$\sigma(\text{exp.})(\text{mb})$	Error(mb)	$\sigma(\text{Com.})(\text{mb})$	$\sigma(\text{Com.} + \text{Pre-com.})(\text{mb})$
	30	-	-	0.09183	0.1713
	33	9.81	2.0	-	-
	35	-	-	10.34	16.6
	36.6	36.3	6.8	-	-
	39.8	36.3	6.8	-	-
	40	-	-	22.92	38.54
	43.4	63.3	12.0	-	-
	45	-	-	46.04	79.19
	48.1	56.2	15.0	-	-
	50	-	-	89.04	168.1

Table: 4.3 Theoretical and Measured Cross-Section for the Reaction  $^{27}_{13}\text{Al}(\alpha, n + 2p)^{28}_{13}\text{Al}$

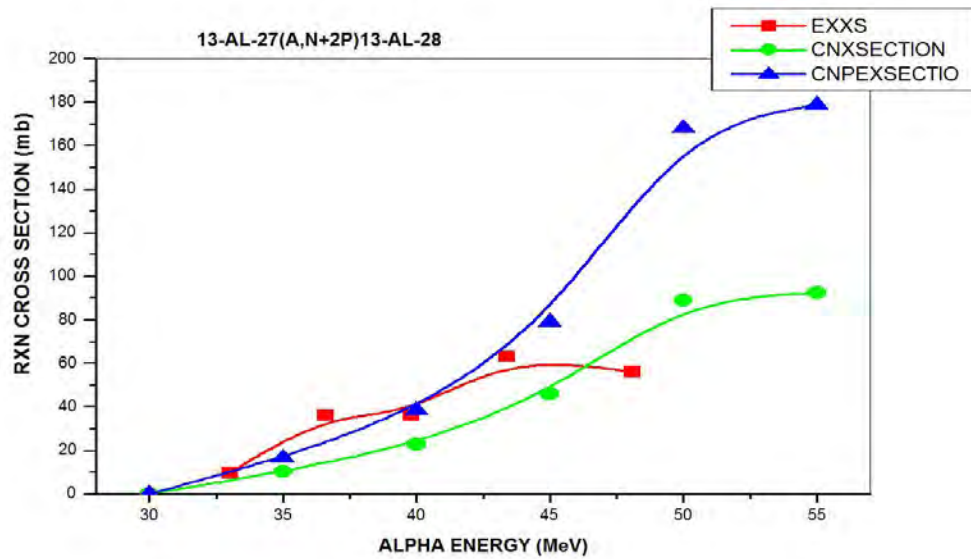


Fig. 4.8 Experimental and Theoretical Excitation Function for the Reaction

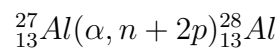


Table (4.3) and fig (4.8) shows the reaction channel under which the evaporation of three nucleons (one neutron and two protons) occur with the residual nucleus of  $^{28}\text{Al}$ . In the energy range from 30MeV to abot 43MeV the experimental values are more closer to

pre-equilibrium theory. After 43 MeV the pre-compound values starts increasing rapidly while experimental value remains nearly constant and is closer to compound nucleus theory.

#### 4.2.4 $^{197}_{79}\text{Au}(\alpha, n + 2p)^{198}_{79}\text{Au}$ Reaction

Projectile			
Energy(MeV)	$\sigma(\text{exp.})(\text{mb})$	$\sigma(\text{Com.})(\text{mb})$	$\sigma(\text{Com.} + \text{Pre} - \text{com.})(\text{mb})$
30	-	0	0
35	-	1.74E-8	9.113E-8
38.4	1.26	-	-
40	-	1.909E-5	6.894E-4
44.2	1.95	-	-
45	-	2.344E-4	0.05552
49.8	3.4	-	-
50	-	6.107E-4	0.5817
55	-	4.334E-4	2.258
55.4	5.9	-	-

Table: 4.4 Theoretical and Measured Cross-Section for the Reaction

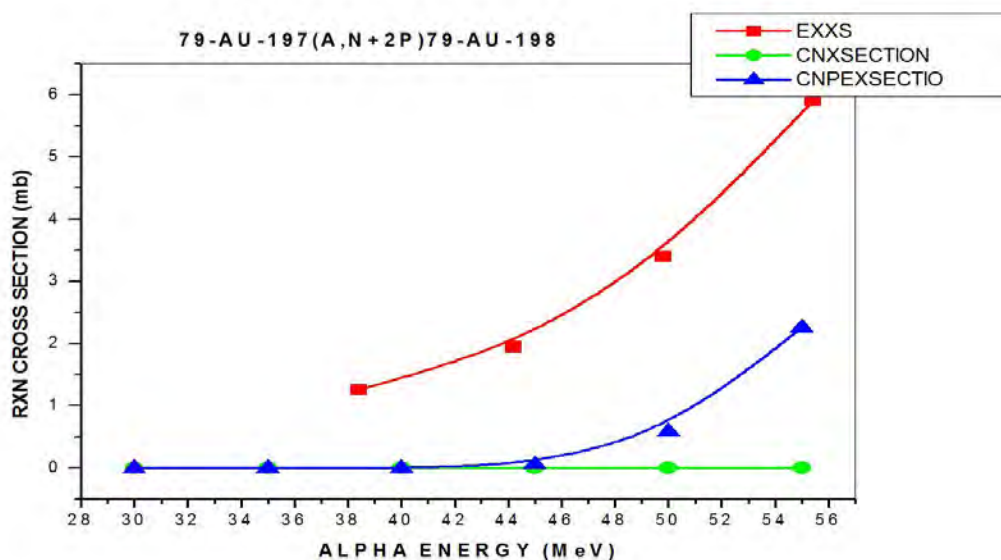
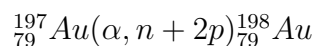
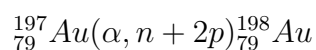


Fig. 4.9 Experimental and Theoretical Excitation Function for the Reaction



From table (4.4) and fig (4.9) the experimental values of excitation function is much higher than the compound nucleus and pre-compound nucleus calculations. This may be the example of stripping of alpha in heavy target and absorption of one neutron while the emission of n+2p.

#### 4.2.5 $^{27}_{13}\text{Al}(\alpha, 2p)^{29}_{13}\text{Al}$ Reaction

Projectile	Energy(MeV)	$\sigma(\text{exp.})(\text{mb})$	Error(mb)	$\sigma(\text{Com.})(\text{mb})$	$\sigma(\text{Com.} + \text{Pre} - \text{com.})(\text{mb})$
	40	-	-	8.238	17.54
	43.2	12.1	-	-	-
	45	-	-	9.384	19.41
	47.9	9.29	0.91	-	-
	50	-	-	8.561	15.29
	54.5	6.92	-	-	-
	55	-	-	8.519	14.43
	59.5	6.28	-	-	-
	60	-	-	6.285	9.443
	65	5.27	-	6.33	8.577
	66.9	4.62 -	-	-	-
	69.5	4,68	-	-	-
	70	-	-	5.332	6.959
	74.4	4.24	-	-	-
	75	-	-	3.806	4.486
	77	3.68	-	-	-
	80	-	-	3.489	3.917
	81.9	3.56	-	-	-
	85	-	-	3.123	3.452
	87.2	2.4	0.26	-	-
	90	-	-	2.086	2.227
	91.1	2.33	-	-	-
	95	-	-	1.798	2.115

Table: 4.5 Theoretical and Measured Cross-Section for the Reaction  $^{27}_{13}\text{Al}(\alpha, 2p)^{29}_{13}\text{Al}$

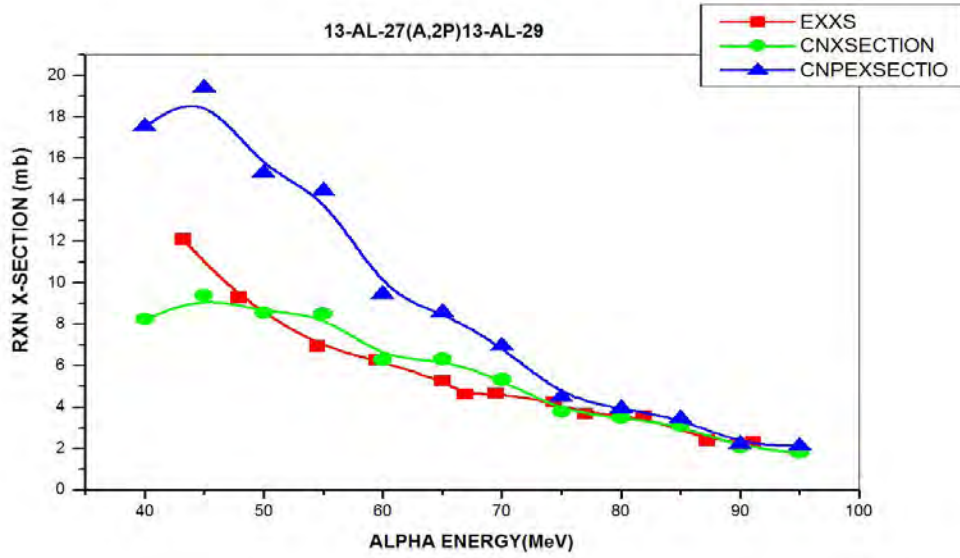
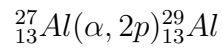


Fig. 4.10 Experimental and Theoretical Excitation Function for the Reaction



The emission of two nucleons (2 protons) is observed in the above reaction channel. The Experimental values of the cross-section for this reaction are closer to compound nucleus calculations up to 75 MeV, while pre-compound calculations are larger but after 75 MeV both compound nucleus and pre-compound nucleus calculation overlap with the experimental values. Thus the reaction channel in this energy range in light nuclei is explained by both the reaction models.

### 4.2.6 $^{197}_{79}\text{Au}(\alpha, 2p)^{199}_{79}\text{Au}$ Reaction

Energy(MeV)	$\sigma(\text{exp.})(\text{mb})$	Error(mb)	$\sigma(\text{Com.})(\text{mb})$	$\sigma(\text{Com.} + \text{Pre} - \text{com.})(\text{mb})$
40	-	-	1.288E-6	9.767E-4
42	0.08	0.02	-	-
45	-	-	7.97E-7	0.01
50	-	-	1.486E-7	0.03141
53	0.19	0.05	-	-
55	-	-	1.509E-8	0.05255
56	0.16	0.04	-	-
60	-	-	1.32E-9	0.06682
62	0.24	0.06	-	-
65	-	-	8.82E-11	0.07202
70	-	-	5.738E-12	0.07392
75	0.24	0.06	3.594E-13	0.07444
80	-	-	9.913E-14	0.06734
85	-	-	6.667E-15	0.06035
90	-	-	2.767E-16	0.05386
91	0.26	0.06	-	-
95	-	-	1.815E-17	0.04789

Table: 4.6 Theoretical and Measured Cross-Section for the Reaction  $^{197}_{79}\text{Au}(\alpha, 2p)^{199}_{79}\text{Au}$

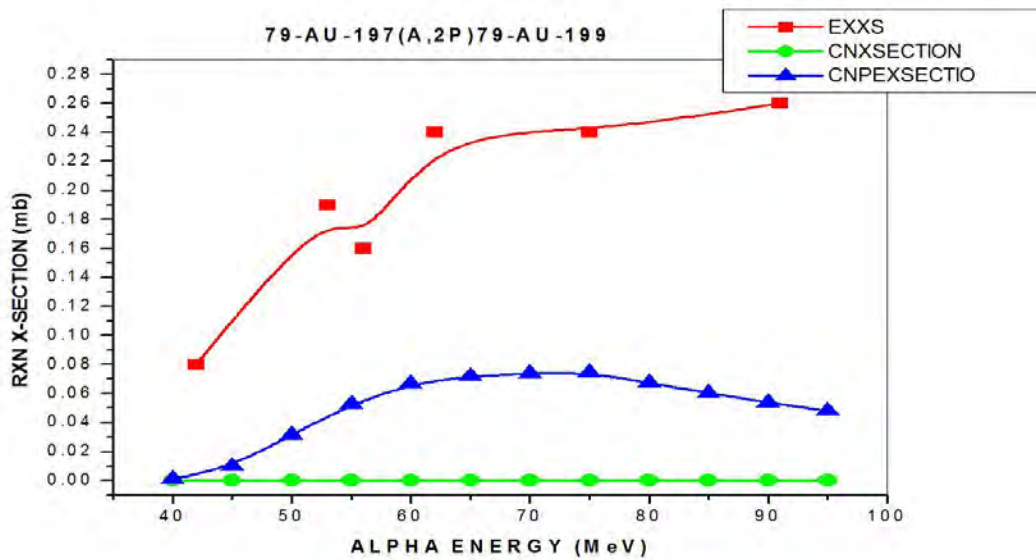
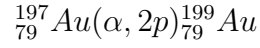


Fig. 4.11 Experimental and Theoretical Excitation Function for the Reaction



In the results presented in table (4.6) and fig (4.11) the experimental result are much higher than the theoretical values calculated from both the models (compound & pre-compound) and goes on increasing with energy. This is the direct proof of stripping reaction in which two neutrons of alpha particle are absorbed by target nuclei and two protons are emitted due to repulsive Coulomb force. This also tells the difference in the ( $\alpha, 2p$ ) reaction in light nuclei and heavy nuclei at the energies under considerations.

#### 4.2.7 ${}_{13}^{27}\text{Al}(\alpha, \alpha + n){}_{13}^{26}\text{Al}$ Reaction

Projectile			
Energy(MeV)	$\sigma(\text{exp.})(\text{mb})$	$\sigma(\text{Com.})(\text{mb})$	$\sigma(\text{Com.} + \text{Pre} - \text{com.})(\text{mb})$
29.5	202	-	-
30	-	118.5	84.3
35	-	245.8	162.4
36.3	227	-	-
40	-	262	161.2
41	162	-	-
45	-	326.6	178.3
50	-	290.1	146
55	-	265.5	118.1
59.2	56	-	-
60	-	264.7	108.9
65	-	207.2	84.09
70	-	184.8	66.4
72.9	67	-	-
75	-	156.7	58.35

Table: 4.7 Theoretical and Measured Cross-Section for the Reaction  ${}_{13}^{27}\text{Al}(\alpha, \alpha + n){}_{13}^{26}\text{Al}$   
The energy error of the above experimental values is 2.5MeV and the data error is 17%.

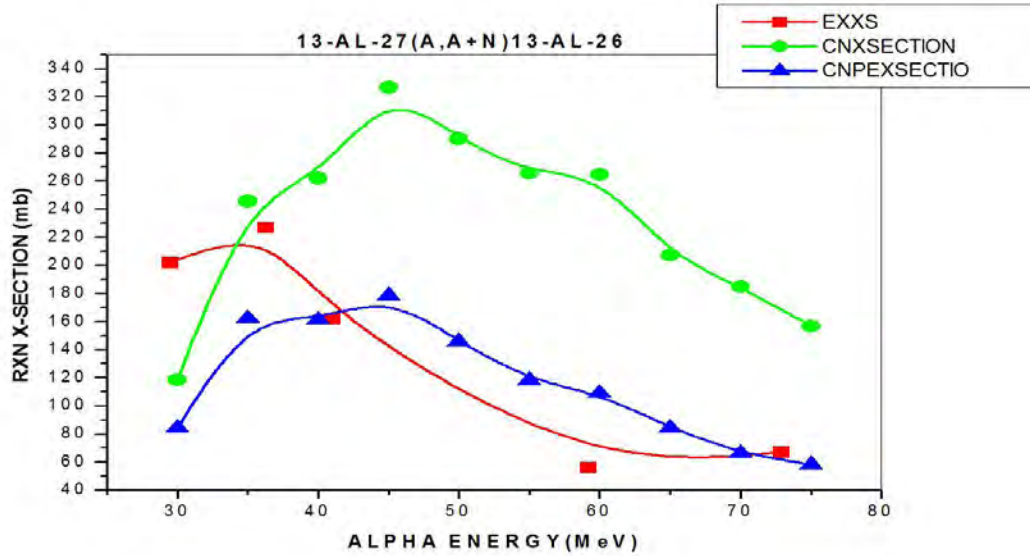
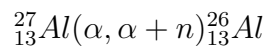


Fig. 4.12 Experimental and Theoretical Excitation Function for the Reaction



The reaction channel for the results indicated in the table (4.7) and Fig. (4.12) is mostly characterized by the pre-equilibrium reaction model for the projectile energy exceeding 40 MeV. The variation between the plots of theoretically calculated pre-equilibrium model reaction and that of the experimental plot is from the experimental energy and data error mentioned above. The major inconsistency happens for the lower energy range (30-40 MeV) where none of the models explain the reaction but compound nucleus theory results are more closer than pre-compound. It is also possible that at low energy of the projectile alpha particle is interacting with surface nucleon and picks up a neutron; no compound system is formed.

#### 4.2.8 $^{197}_{79}\text{Au}(\alpha, \alpha + n)^{196}_{79}\text{Au}$ Reaction

Projectile			
Energy(MeV)	$\sigma(\text{exp.})(\text{mb})$	$\sigma(\text{Com.})(\text{mb})$	$\sigma(\text{Com.} + \text{Pre} - \text{com.})(\text{mb})$
25	-	0.00328	0.00318
25.1	0.55	-	-
29.8	2.4	-	-
30	-	0.03526	0.05619
30.6	3.8	-	-
34.7	14.5	-	-
35	-	0.1143	0.3212
35.2	10.9	-	-
39.2	26	-	-
40	33	0.05592	0.4924
45	-	0.008	0.4757
46	52	-	-
50	-	7.799E-4	0.2545
50.5	71	-	-
55	-	3.513E-4	0.1704
55.6	89	-	-
60	-	0.00665	0.2124
61.5	95	-	-
65	-	0.03469	0.6633
65.4	104	-	-
70	-	0.07704	2.113
70.2	106	-	-
75	-	0.0977	5.81

Table: 4.8 Theoretical and Measured Cross-Section for the Reaction

$$^{197}_{79}\text{Au}(\alpha, \alpha + n)^{196}_{79}\text{Au}$$

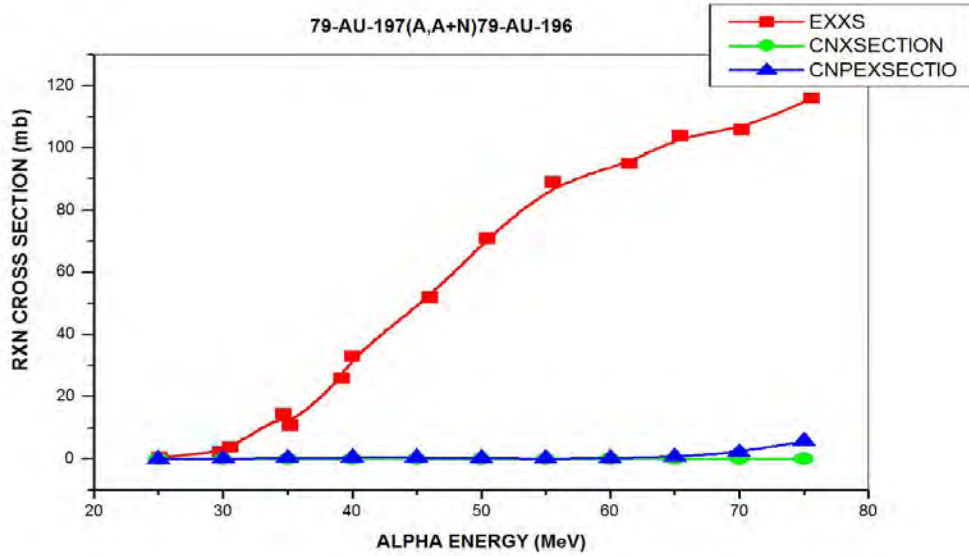
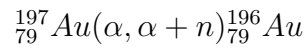


Fig. 4.13 Experimental and Theoretical Excitation Function for the Reaction



The theoretically calculated reaction cross section calculated using both compound and Pre-compound theory are nearly equal and very-very small. Up to 30 MeV the experimental value is explained by both the theories: table (4.8) and fig. (4.13). After 30 MeV the experimental value of cross section starts increasing and goes on increasing very rapidly. This shows that at these energies in the heavy nuclei the reaction takes place via the direct reaction channel, while with the light nuclei (Al) this was pre-equilibrium mechanism. In the energy range specified here, the projectile particle ( $\alpha$ ) picks up one nucleon (neutron) from the target nucleus ( ${}^{197}\text{Au}$ ) and pick up direct reaction takes place. This shows the presence of larger number of surface nucleons in heavier nuclei.

# Chapter 5

## Conclusion

Results of the present work are summarized on the plots of Fig. 4.6 to Fig. 4.13, where experimental and theoretical best fit excitation function graphs for;  ${}^{27}_{13}\text{Al}(\alpha, n){}^{30}_{15}\text{P}$ ,  ${}^{27}_{13}\text{Al}(\alpha, 2p){}^{29}_{13}\text{Al}$ ,  ${}^{27}_{13}\text{Al}(\alpha, n+2p){}^{28}_{13}\text{Al}$ ,  ${}^{27}_{13}\text{Al}(\alpha, \alpha+n){}^{26}_{13}\text{Al}$ ;  ${}^{197}_{79}\text{Au}(\alpha, n){}^{200}_{81}\text{Tl}$ ,  ${}^{197}_{79}\text{Au}(\alpha, 2p){}^{199}_{79}\text{Au}$ ,  ${}^{197}_{79}\text{Au}(\alpha, n+2p){}^{198}_{79}\text{Au}$  and  ${}^{197}_{79}\text{Au}(\alpha, \alpha+n){}^{196}_{79}\text{Au}$ . As mentioned earlier the objective of this thesis is to evaluate the excitation functions of the two target nuclide; the light  ${}^{27}\text{Al}$  nucleus and the heavy  ${}^{197}\text{Au}$  nucleus separately and to compare the results of both nuclides in different reaction channels with different energy range. Accordingly the following analysis was done.

Comparing the reactions of both target nuclei in reaction channels discussed under 4.2.1 and 4.2.2 at the higher energy range for neutron emission reaction, it is observed that for light ( ${}^{27}\text{Al}$ ) nucleus the reaction can not be explained neither by pre-equilibrium nor by the equilibrium model. The experimental value falls to zero rapidly and in the case of heavy nucleus ( ${}^{197}\text{Au}$ ), in the higher energy region ( $> 13\text{MeV}$ ) the graph of theoretically calculated pre-equilibrium excitation function approaching the result of the experimental value obtained from the data source. Comparative analysis between the light ( ${}^{27}\text{Al}$ ) and heavy ( ${}^{197}\text{Au}$ ) target nuclei for the emission of n+2p reaction shown in sections 4.2.3 and 4.2.4, for the heavy nucleus this reaction channel is totally explained by stripping direct reaction, while for the light target nucleus ( ${}^{27}\text{Al}$ ) based on the energy of the projectile it is either the compound nucleus model or the pre-equilibrium decay .

From the discussion under 4.2.5 and 4.2.6 for 2p emission reaction significant differences were observed between the light  $^{27}\text{Al}$  and the heavy  $^{197}\text{Au}$  target nuclei. In heavy nucleus, at all the energies it is stripping of alpha particle with the emission of 2p and absorption of 2n by the target nucleus, while in the case of light nucleus ( $^{27}\text{Al}$ ) the reaction channel is governed by both compound nucleus and pre-compound models for energy exceeding 75MeV and compound nucleus model for lower energy range. From the discussion of sections 4.2.7 and 4.2.8 for  $(\alpha, \alpha + n)$  channel in heavy nucleus ( $^{197}\text{Au}$ ) the reaction mechanism is direct pick up reaction while in the light nuclei ( $^{27}\text{Al}$ ) though there is inconsistency at lower energy range, the reaction channel is mostly characterized by the pre-equilibrium reaction model for the projectile energy exceeding 40 MeV.

# References

- [1] Nuclear Physics Principles and Applications, John Lilly: John Wiley & Sons Ltd, 2001.
- [2] Introductory Nuclear Physics, Kenneth S. Krane, John Wiley & sons, 1988.
- [3] IAEA EXFOR Nuclear Data Library, <https://www-nds.iaea.org/exfor/exfor.htm>
- [4] Emmeric Dupont\*, Journal of the Korean Physical Society, Vol.59, No.2, August 2011, pp.1333-1336.
- [5] Google Wikipedia, [en.wikipedia.org/wiki/](http://en.wikipedia.org/wiki/)
- [6] Significant amount of Pre-equilibrium contribution in the  $\alpha + 93 \text{ Nb}$  systems at energies 18-40 MeV. F.K. Amanuel, B.A. Zelalem, A. K. Chaubey, Avinash Agarwal, I.A.Rizvi, Chinese Journal of Physics, vol 49, 4, page 884 (2011).
- [7] Hyeong Il Kim\* and Young-Ouk Lee, Journal of the Korean Physical Society, Vol.52, No.3, March 2008, pp.837-842.
- [8] Introductory Nuclear Physics, P.E. Hodgson, E. Gadioli and E.GadioliErba: Oxford University press, 2003.
- [9] Direct Nuclear Reaction, Norman K Glendenning, Lawrence Berkeley national Laboratory, USA, 2004.
- [10] Nuclear Physics Experimental and Theoretical, 2nd Edition, H S Hans: New Academic Science, 2011.
- [11] V.F. Weisskopf, Mod.Phys.29,174 (1959).
- [12] Fundamentals In Nuclear Physics, Jean-Louis, Basdevant, James Rich, Michel Spiro, Springer Science+Business Media, Inc. 2005.
- [13] TALYS: Comprehensive nuclear reaction modelling, A.J. Koning et al., International Conference on Nuclear Data for Science and Technology, American Institute of Physics,

2005.

[14] R.K.Y. Singh et al., Chinese Journal of Physics 39, 4 (2001).

[15] Excitation function studies of alpha induced reactions for niobium and pre-equilibrium effects. Avinash Agarwal, I. A. Rizvi, and A. K. Chaubey Physical Review C 65, 34605, (2002).

[16] Non equilibrium emission of neutrons in alpha induced reactions in holmium Avinash Agarwal, I.A.Rizvi and A.K. Chaubey Canadian Journal of Physics , vol. 86(3),495, (2008).

[17] Comparison between pre-equilibrium and intra nuclear cascade model at intermediate energy, Yu. N. Shubin, V. P. Lunev, A. Yu. Konobeyev and Yu. A. Korovin, Institute of physical and power engineering, Obninsk, Russia.

[18] Measurement and analysis of excitation functions for alpha induced reactions with rubidium. Avinash Agarwal, M. K. Bhardwaj, I. A. Rizvi, and A. K. Chaubey Indian Journal of Pure and Applied Physics, Vol. 41, 829, (2003).

[19] Pre-equilibrium nuclear reactions: An introduction to classical and quantum-mechanical models, A.J. Koning, J.M. Akkerman, Netherlands Energy Research Foundation ECN, BU-Nuclear research, The Netherlands.

[20] Computer Code COMPLET, Prof. Dr. J. Ernst, Institute Fuer Strahlen-UND Kernphysik, Nussallee 14-16, D 53115, Bonn, F.R. Germany

[21] Calculation of Level Density Parameter of Nuclear Reaction Using Neural Network, Rizal Kurniadi et.al, Indonesian Journal of Physics, Vol 20 No. 3, October 2009.

[22] H. A. Bethe, Rev. Mod. Phys. 9(1937)69.

### **Declaration**

This thesis is my original work, has not been presented for a degree in any other University and that all the sources of material used for the thesis have been dully acknowledged.

Ejigu Kebede

Signature:—————

Addis Ababa University, June 2014

This thesis has been submitted for examination with my approval as University advisor.

Prof. A.K. Chaubey

Signature:—————